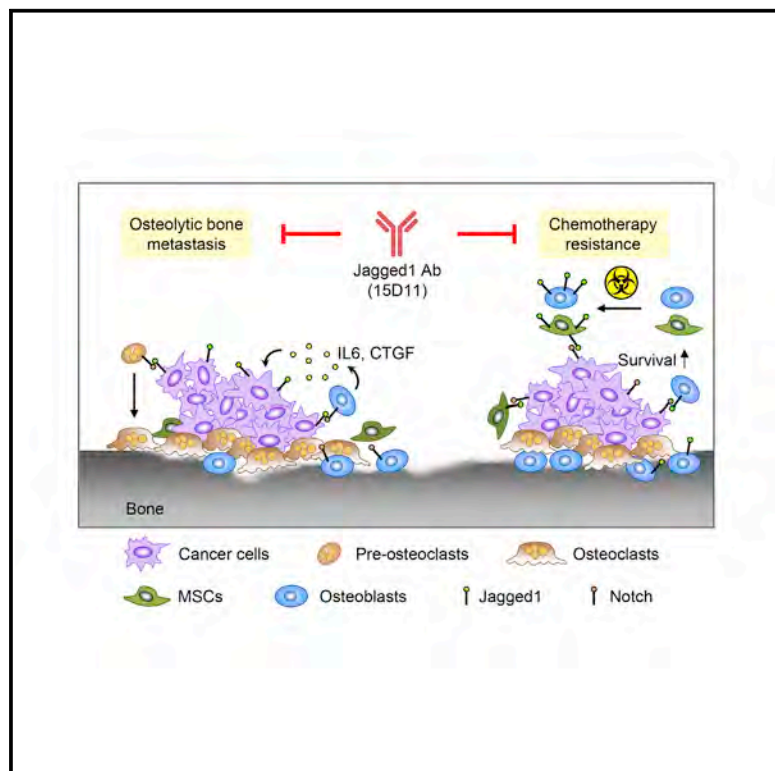# Cancer Cell

Therapeutic Antibody Targeting Tumor- and Osteoblastic Niche-Derived Jagged1 Sensitizes Bone Metastasis to Chemotherapy

Graphical Abstract

Authors

Hanqiu Zheng, Yangjin Bae,
Sabine Kasimir-Bauer, ...,
Angela Coxon, Brendan Lee,
Yibin Kang

Correspondence

blee@bcm.edu (B.L.),
ykang@princeton.edu (Y.K.)

In Brief

Zheng et al. develop 15D11, a fully human monoclonal antibody to Jagged1, which inhibits Jagged1 on breast cancer cells as well as blocking metastasis-promoting effects of osteoblast-derived Jagged1 induced by chemotherapy. 15D11 reduces bone metastasis and sensitizes metastases to chemotherapy in mouse models of breast cancer.

Highlights

- Jagged1 antibody 15D11 reduces bone metastasis without significant side effects

- Chemotherapy induces tumor-protecting Jagged1 in osteoblasts

- Transgenic expression of Jagged1 in osteoblasts promotes bone metastasis

- 15D11 sensitizes bone metastasis to chemotherapy

CrossMark

CellPress

CellPress

Therapeutic Antibody Targeting Tumor- and Osteoblastic Niche-Derived Jagged1 Sensitizes Bone Metastasis to Chemotherapy

Hanqiu Zheng,[1,11,12] Yangjin Bae,[2,12] Sabine Kasimir-Bauer,[3] Rebecca Tang,[1] Jin Chen,[1] Guangwen Ren,[1] Min Yuan,[1] Mark Esposito,[1] Wenyang Li,[1] Yong Wei,[1] Minhong Shen,[1] Lanjing Zhang,[4,10] Nikolai Tupitsyn,[5] Klaus Pantel,[6] Chadwick King,[7] Jan Sun,[7] Jodi Moriguchi,[7] Helen Toni Jun,[8] Angela Coxon,[7] Brendan Lee,[2,*] and Yibin Kang[1,9,13,*]
[1]Department of Molecular Biology, Princeton University, Washington Road, LTL 255, Princeton, NJ 08544, USA
[2]Department of Molecular and Human Genetics, Baylor College of Medicine, One Baylor Plaza, Room R814 BCM225, Houston, TX 77030, USA
[3]Department of Gynecology and Obstetrics, University Hospital Essen, Essen, Germany
[4]Department of Pathology, University Medical Center of Princeton, Plainsboro, NJ, USA
[5]Laboratory of Hematopoiesis Immunology, Cancer Research Center, Moscow, Russia
[6]Department of Tumor Biology, University Medical Center Hamburg-Eppendorf, Center of Experimental Medicine, Hamburg, Germany
[7]Oncology Research, Amgen Inc., Thousand Oaks, CA 91320, USA
[8]MabVax Therapeutics Holdings, Inc., San Diego, CA 92121, USA
[9]Cancer Metabolism and Growth Program, Rutgers Cancer Institute of New Jersey, New Brunswick, NJ 08903, USA
[10]Rutgers Cancer Institute of New Jersey, New Brunswick, NJ, USA
[11]Present address: Department of Basic Medical Sciences, School of Medicine, Tsinghua University, Beijing, China
[12]These authors contributed equally
[13]Lead Contact
*Correspondence: blee@bcm.edu (B.L.), ykang@princeton.edu (Y.K.)
https://doi.org/10.1016/j.ccell.2017.11.002

SUMMARY

Bone metastasis is a major health threat to breast cancer patients. Tumor-derived Jagged1 represents a central node in mediating tumor-stromal interactions that promote osteolytic bone metastasis. Here, we report the development of a highly effective fully human monoclonal antibody against Jagged1 (clone 15D11). In addition to its inhibitory effect on bone metastasis of Jagged1-expressing tumor cells, 15D11 dramatically sensitizes bone metastasis to chemotherapy, which induces Jagged1 expression in osteoblasts to provide a survival niche for cancer cells. We further confirm the bone metastasis-promoting function of osteoblast-derived Jagged1 using osteoblast-specific Jagged1 transgenic mouse model. These findings establish 15D11 as a potential therapeutic agent for the prevention or treatment of bone metastasis.

INTRODUCTION

Breast cancer is the most common female malignancy and the second leading cause of cancer-related death in the United States. Among late-stage breast cancer patients, more than 70% suffer from bone metastasis, which is often accompanied by severe bone pain, fracture, and potentially lethal complications such as hypercalcemia (Weilbaecher et al., 2011). Although radiotherapy, chemotherapy, and anti-osteolytic agents such as bisphosphonate and RANKL antibody denosumab can reduce morbidity associated with bone metastasis, these treatments often do not significantly extend the survival time of the patients

Significance

Current treatments for bone metastasis often reduce skeletal-related events without significant reduction of tumor burden or survival benefit for patients. Furthermore, bone metastasis is particularly refractory to chemotherapy. While γ-secretase inhibitors have therapeutic efficacy against bone metastasis in preclinical models, the high gastrointestinal tract toxicity of these agents prevented their further clinical development. 15D11 is a fully human monoclonal antibody against Jagged1 with minimal toxicity and excellent therapeutic efficacy against bone metastasis. Importantly, by targeting tumor-protective osteoblastic Jagged1 induced by chemotherapy, 15D11 synergizes with chemotherapy to reduce bone metastasis burden by more than 100-fold and dramatically reduces metastatic relapse to bone from primary tumors. These results indicate broad potential applications of 15D11 for bone metastasis prevention or treatment.
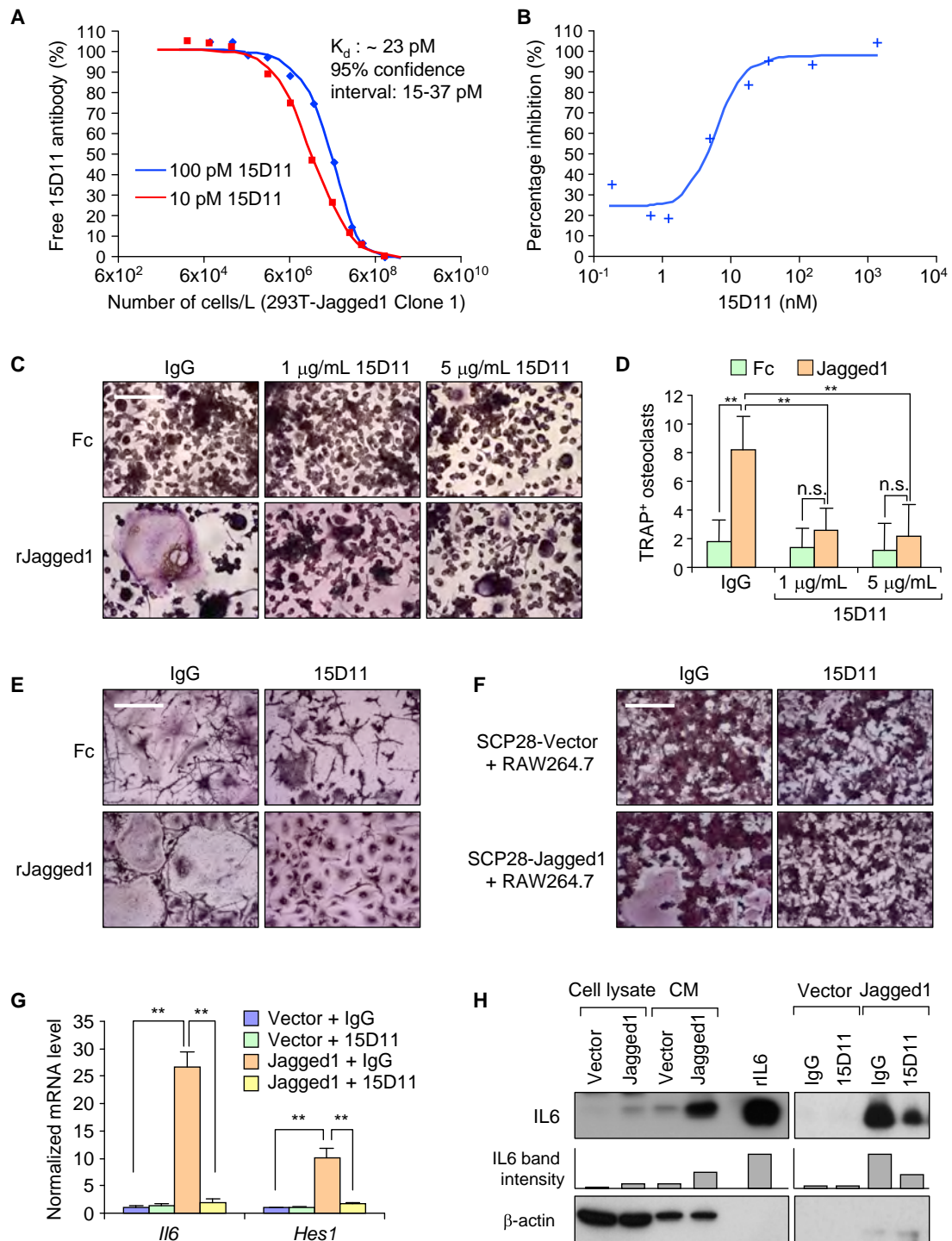
CrossMark

Figure 1. Characterization of Fully Human Monoclonal Antibodies against Jagged1

(A) Kinetic exclusion assay for binding of 15D11 with murine Jagged1 protein. Increasing number (1.5×10^2 to 9×10^6) of 293T cells with murine Jagged1 expression (clone no. 1) were added into the solution with fixed amount of 15D11 antibody (10 or 100 pM) and remaining amount of antibody in the liquid was determined after 4 hr.

(B) A Notch reporter luciferase assay was used to determine half maximal inhibitory concentration for 15D11 in Jagged1-induced Notch activation. Human TE671 expressing a multimerized 7XCSL-responsive element upstream of a minimal promoter (Notch reporter) were co-cultured with HEK293 expressing Jagged1. 15D11 (0.07–1,333.4 nM) was added to the cells for 2 days. Luciferase signal was quantified. The percent inhibition was calculated relative to signals of reactions lacking 15D11 and 293T co-culture.

(legend continued on next page)

or provide a cure (Weilbaecher et al., 2011), as metastatic cancers often acquire resistance to these treatments.

Tumor-stromal interaction plays a major role in promoting bone metastasis of breast cancer (Weilbaecher et al., 2011). The bone microenvironment contains a great variety of stromal cell types, such as osteoblasts, osteoclasts, mesenchymal stem cells (MSCs), and hematopoietic cells. While previous research has focused on the cross-communication between breast cancer cells and bone-resorbing osteoclasts, the contributions of other stromal cell types to bone metastasis are less studied. Among the supporting stromal cells, bone-building osteoblasts have recently been shown to constitute an osteogenic niche that is critical for the survival and colonization of disseminated tumor cells (DTCs) in the bone (Shiozawa et al., 2011; Wang et al., 2015). Despite this recent progress, our molecular understanding of the interaction between tumor cells and osteoblastic cells in the bone niche remain largely incomplete. For example, how such tumor-niche interactions contribute to the resistance of metastatic breast cancer to standard bone metastasis treatments, such as chemotherapy, remains poorly understood.

In human breast cancer, elevated expression of Jagged1 and Notch1, but not other Notch pathway ligands or receptors, is significantly associated with poor prognosis (Reedijk et al., 2005; Sethi et al., 2011). Our previous study identified tumor-derived Jagged1 as a bone metastasis-promoting factor by activating Notch signaling in osteoblasts to increase the production of interleukin-6 (IL6) and connective tissue growth factor (TGF), which feeds back to tumor cells to promote proliferation and survival. Meanwhile, Jagged1 stimulates osteoclastogenesis and bone degradation, leading to the release of bone-derived growth factors including TGF-β, a potent inducer of Jagged1 expression in tumor cells, thus forming a positive feedback cycle (Sethi et al., 2011).

Besides Jagged1's role in tumor-stromal interaction during bone metastasis progression, tumor- or stromal-derived Jagged1 has also been reported to induce angiogenesis, invasion, therapy resistance, and cancer stem cell renewal in lymphoma, colorectal cancer, and many other cancer types (Li et al., 2014). Endothelium-derived Jagged1 promotes Notch activation in B cell lymphoma, leading to extra-nodal invasion and chemoresistance (Cao et al., 2014). In colorectal cancer, a soluble form of Jagged1 derived from endothelial cells induces a cancer stem cell-like phenotype in colorectal cancer (Lu et al., 2013). These multi-functional roles of Jagged1 in different cancer types support the development of Jagged1 targeting therapeutics for cancer treatments.

Several therapeutic strategies have been developed to target the Notch signaling pathway. Most of the inhibitors were designed to target γ-secretase, which mediates the proteolytic cleavage of Notch receptors to generate a signal-transducing Notch intracellular domain, a necessary step in Notch pathway activation upon ligand binding (Rizzo et al., 2008). However, γ-secretase inhibitor (GSI) has been reported to induce severe gastrointestinal (GI) tract toxicity (Imbimbo, 2008), preventing further clinical development of this class of inhibitors. Targeting individual Notch receptor or ligand can potentially achieve therapeutic effect without causing severe GI tract toxicity.

RESULTS

Generation and Characterization of a Fully Human Monoclonal Antibody Against Jagged1

We utilized the XenoMouse technology to generate fully human monoclonal antibodies against Jagged1. These mice have the endogenous mouse immunoglobulin loci inactivated and large transgenes introduced, which are capable of recombination and fully human antibody repertoire development (Mendez et al., 1997). In brief, we immunized XenoMouse animals, including strains XMG2KL and XMG4KL (Kellermann and Green, 2002), with Chinese hamster ovary cells transiently expressing human Jagged1 to generate large panels of antibodies. Cell-based fluorometric microvolume assay technology was used to analyze the specific binding of these antibodies to cell surface human Jagged1 protein. These antibodies were then counter screened to exclude cross-reactive binding to other major Notch ligands, including human Jagged2 and Dll4 (Figure S1A). To identify a suitable antibody antagonist that could be used for murine *in vivo* studies, the most potent blockers of the Notch receptor interaction were then further assayed for cross-reactive binding to murine Jagged1. Antibody clone 15D11 is of particularly high affinity to the murine Jagged1 protein, with an approximate dissociation constant (K_D) of 23 pM in the enzyme kinetic exclusion assay (KinExA) (Figure 1A). Using a Notch luciferase reporter assay, we determined that 15D11 has a half maximal inhibitory concentration of 3.63 nM to human Jagged1 and 14.07 nM to murine Jagged1 (Figure 1B and data not shown).

When administered *in vivo* (10 mg/kg, twice a week), 15D11 displayed minimal general toxicity based on body weight

(C) RAW264.7 pre-osteoclast cells were seeded on Fc- or recombinant Jagged1-coated plates in the presence of 5 ng/mL RANKL and the indicated concentrations of IgG or 15D11. Cells were cultured for 5–7 days before fixing for TRAP staining to visualize multi-nucleated mature osteoclasts.

(D) Quantification of TRAP$^+$ osteoclasts per field from (C). Data are presented as mean ± SEM. n = 3. **p < 0.01 by Student's t test. n.s., not significant.

(E) SCP28-Vector or SCP28-Jagged1 cells were co-cultured with RAW264.7 cells in the presence of 5 ng/mL RANKL and 1 μg/mL IgG or 15D11. Cells were cultured for 5–7 days before fixing for TRAP staining to visualize multi-nucleated mature osteoclasts.

(F) Primary bone marrow cells were flushed from tibias of 4–6-week-old WT FVB mice and plated for 24 hr, after which the non-adherent cells were collected and cultured in M-CSF (50 ng/mL) for 2 days and then co-cultured with SCP28-Vector or SCP28-Jagged1 in the presence of RANKL (20 ng/mL) and 1 μg/mL IgG or 15D11. Cells were allowed to differentiate into osteoclasts for additional 4–5 days before fixing and TRAP staining.

(G) mRNA expression of mouse *Il6* and *Hes1* in MC3T3 cells co-cultured with SCP28-Vector control or SCP28-Jagged1 cells, treated with either IgG control or 15D11. Primers used in this experiment were specifically designed to only detect mouse genes, but not human genes. n = 3. **p < 0.01 by Student's t test. Data are presented as mean ± SEM.

(H) Expression of IL6 protein in cell lysate and conditioned medium (CM) taken from MC3T3 cells co-cultured with SCP28-Vector or SCP28-Jagged1 cells (left). Recombinant IL6 served as positive control. IL6 protein expression in CM from MC3T3 cells co-cultured with SCP28-Vector or SCP28-Jagged1 cells, treated with either IgG control or 15D11 antibody (right). β-Actin served as loading control. Bars below the IL6 immunoblots represent relative bone density of IL6 as quantified by ImageJ software. Scale bars, 100 μm in (C, E, and F). See also Figure S1.

measurement, in contrast to significant weight loss of mice treated with GSI (Figure S1B). H&E staining and Alcian blue staining revealed no obvious GI tract toxicity after 15D11 treatment, compared with significant goblet cell metaplasia seen in GSI-treated animals (Figures S1C and S1D). To analyze liver toxicity, we measured the activity of alanine aminotransferase (ALT) and aspartate aminotransferase (AST) in the sera of these mice after the respective drug treatments. As a positive control, CCl$_4$ treatment induced dramatic increase of ALT and AST activity (Figures S1E and S1F), while no change was observed after 15D11 or GSI treatment. A complete blood count test further indicated no significant hematologic toxicity of 15D11 (Figure S1G). Analysis of T cell population and activation status also did not reveal any difference between the immunoglobulin G (IgG) or 15D11 treatment groups (Figures S1H–S1K). Taken together, these results indicate that 15D11 is a specific Jagged1-targeting agent with excellent safety profile for *in vivo* application.

Our previous study demonstrated that tumor-derived Jagged1 promotes the differentiation of monocytic pre-osteoclast into mature osteoclasts (Sethi et al., 2011). We developed an *in vitro* assay to test the potential inhibitory effect of 15D11 on Jagged1-dependent osteoclastogenesis. RAW264.7, a monocyte/macrophage cell line with the ability to differentiate into osteoclasts, was seeded on either Fc-coated or recombinant Jagged1 (rJagged1)-coated plates with a low level of RANKL (5 ng/mL), a concentration that is not sufficient to induce osteoclast differentiation (Ell et al., 2013). Within 5 days, large multi-nuclear mature osteoclasts were generated on rJagged1-coated plates, but only limited numbers can be seen on Fc-coated plates. Furthermore, such Jagged1-dependent osteoclast differentiation was completely blocked by 15D11 (Figures 1C and 1D). Similar results were observed when using bone marrow-derived primary pre-osteoclasts in the assay (Figures 1E and S1L). To more closely mimic osteoclastogenesis induced by tumor-derived Jagged1, we co-cultured RAW264.7 cells with SCP28 cells, an MDA-MB-231 derivative cell line with moderate bone metastatic ability that has been stably labeled with luciferase and GFP (Kang et al., 2003), with or without stable overexpression of Jagged1. Administration of 15D11 also inhibited osteoclast differentiation in this co-culture assay (Figures 1F and S1M).

Another previously reported mechanism for tumor-derived Jagged1 to promote bone metastasis is through increasing IL6 production from osteoblasts (Sethi et al., 2011). As reported previously, co-culture of SCP28 with the mouse MC3T3 osteoblast cell line led to elevated expression of IL6 in a Jagged1-dependent manner (Figures 1G and 1H). Administration of 15D11 in tumor-osteoblast co-culture significantly repressed the expression of the Notch-induced gene *Hes1* (detected by species-specific qRT-PCR) (Figure 1G), as well as IL6 expression at both the mRNA and protein levels (Figures 1G and 1H). Taken together, these *in vitro* experiments confirm that 15D11 effectively blocks Jagged1-Notch signaling activities that are important for bone metastasis development.

15D11 Antibody Attenuates Bone Metastasis of Jagged1-Expressing Tumor Cells

To evaluate the therapeutic effect of 15D11 on bone metastasis, we turned to a well-established xenograft model for bone metastasis by using SCP28 cells. SCP28 has a low basal level of

Jagged1 expression, and ectopic overexpression of Jagged1 in SCP28 has been demonstrated to enhance its bone metastatic ability (Sethi et al., 2011). Tumor cells were inoculated via intracardiac (IC) injection into athymic nude mice to generate bone metastasis. We initiated the 15D11 antibody treatment 1 day before tumor cell injection and continued the treatment twice a week. Bone metastasis was monitored by weekly bioluminescence imaging (BLI) until mice were euthanized at the end of the experiment (~5 weeks) for histopathological analysis (Figure 2A). We also used the decoy receptor for RANKL, OPG-Fc (equivalent to clinically approved RANKL blocking antibody denosumab), to block osteoclast differentiation as the positive control in the experiment. Jagged1 overexpression led to a significant increase in bone metastasis burden (Figures 2B and 2C), consistent with our previous report (Sethi et al., 2011). BLI analysis revealed an ~5-fold decrease in SCP28-Jagged1 bone metastasis in mice treated with 15D11 compared with the IgG control group. As expected, OPG-Fc treatment also decreased the bone metastasis burden of mice (Figures 2B and 2C). X-ray imaging of the hindlimbs of mice injected with SCP28-Jagged1 revealed significantly more osteolytic areas compared with mice injected with the control SCP28 cells, a phenotype that can be reversed by 15D11 treatment (Figures 2B and 2D). While OPG-Fc treatment also protected bone from osteolysis, it also led to an abnormal increase of the trabecular bone density, as observed by X-ray and microcomputer tomography (μCT) analysis (Figures 2D and 2E; Movies S1–S4). Consistently, tartrate-resistant acid phosphatase (TRAP) immunostaining of bone sections indicated an almost complete absence of osteoclasts in mice treated with OPG-Fc (Figure 2E). Interestingly, while Jagged1-overexpressing SCP28 promoted the recruitment of mature osteoclasts in the bone lesions, a considerable number of osteoclasts can still be observed in mice treated with 15D11 (Figures 2E and S2A). Importantly, there was no abnormal increase of trabecular bone density in 15D11-treated animals, in contrast to OPG-Fc-treated mice (Figure 2E). Taken together, these results suggest that 15D11 inhibits pathological activation of osteoclasts by tumor-derived Jagged1, but spares normal osteoclast activities needed to maintain normal bone homeostasis.

To test the therapeutic effect of 15D11 on established bone metastasis, we used the SCP2 cell line, an extremely aggressive bone metastatic variant of MDA-MB-231 with a high level of endogenous Jagged1 expression (Sethi et al., 2011). The SCP2 cells rapidly generated multiple osteolytic bone metastases within 1 week after IC injection into nude mice, which often results in mortality within 4 weeks. We initiated twice-weekly injection of 15D11 1 week after IC injection of SCP2 cells when bone metastases were well established (Figure S2B). In this model of late treatment of aggressive bone metastasis, we detected a trend of reduced bone metastasis by either 15D11 or OPG-Fc treatment alone compared with the control group (Figures S2C and S2D), although neither of them reach statistical significance at the endpoint of the experiment (4 weeks) when the mice succumbed to metastatic cancers. Combinatory treatment of 15D11 and OPG-Fc resulted in a significant ~5-fold decrease of bone metastasis 3 weeks after the initiation of treatments, indicating the benefit of targeting two different molecular mediators of bone metastasis (Figures S2C and S2D). Similar to
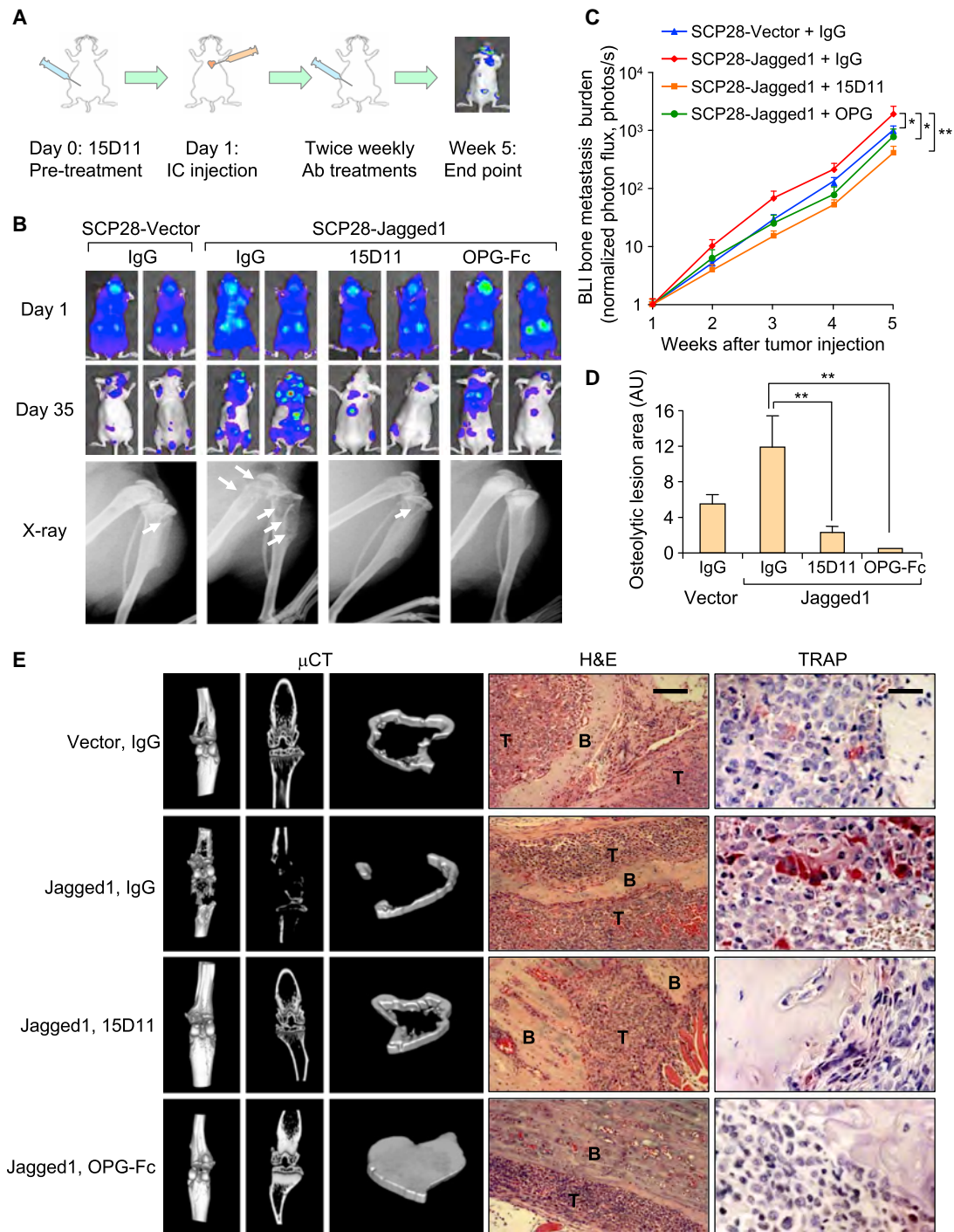
Figure 2. 15D11 Inhibits Tumor-Derived Jagged1-Dependent Bone Metastasis

(A) Schematic representation of the experiment. 10^5 tumor cells were IC injected into each mouse. Mice were treated 1 day before the tumor cell injection and continued twice a week at the dosage of 10 mg/kg for IgG/15D11, and 3 mg/kg for OPG-Fc.

(B) Representative BLI and X-ray images on day 1 immediately after the IC injection and on day 35 at the endpoint of the experiment. Arrows indicate osteolytic bone areas.

(C) Quantification of bone metastasis burden each week based on BLI imaging from the experiment. n = 10 per group; data presented as mean ± SEM. *p < 0.05 and **p< 0.01 by Mann-Whitney test.

(D) Quantification of osteolytic lesions on day 35. n = 8 per group; data presented as mean ± SEM. **p < 0.01 by Student's t test.

(E) Representative μCT, H&E staining, and TRAP staining images from the experiment. T, tumor; B, bone. Scale bars, 100 μm for H&E and 25 μm for TRAP. See also Figures S2 and S3 and Movies S1–S4.
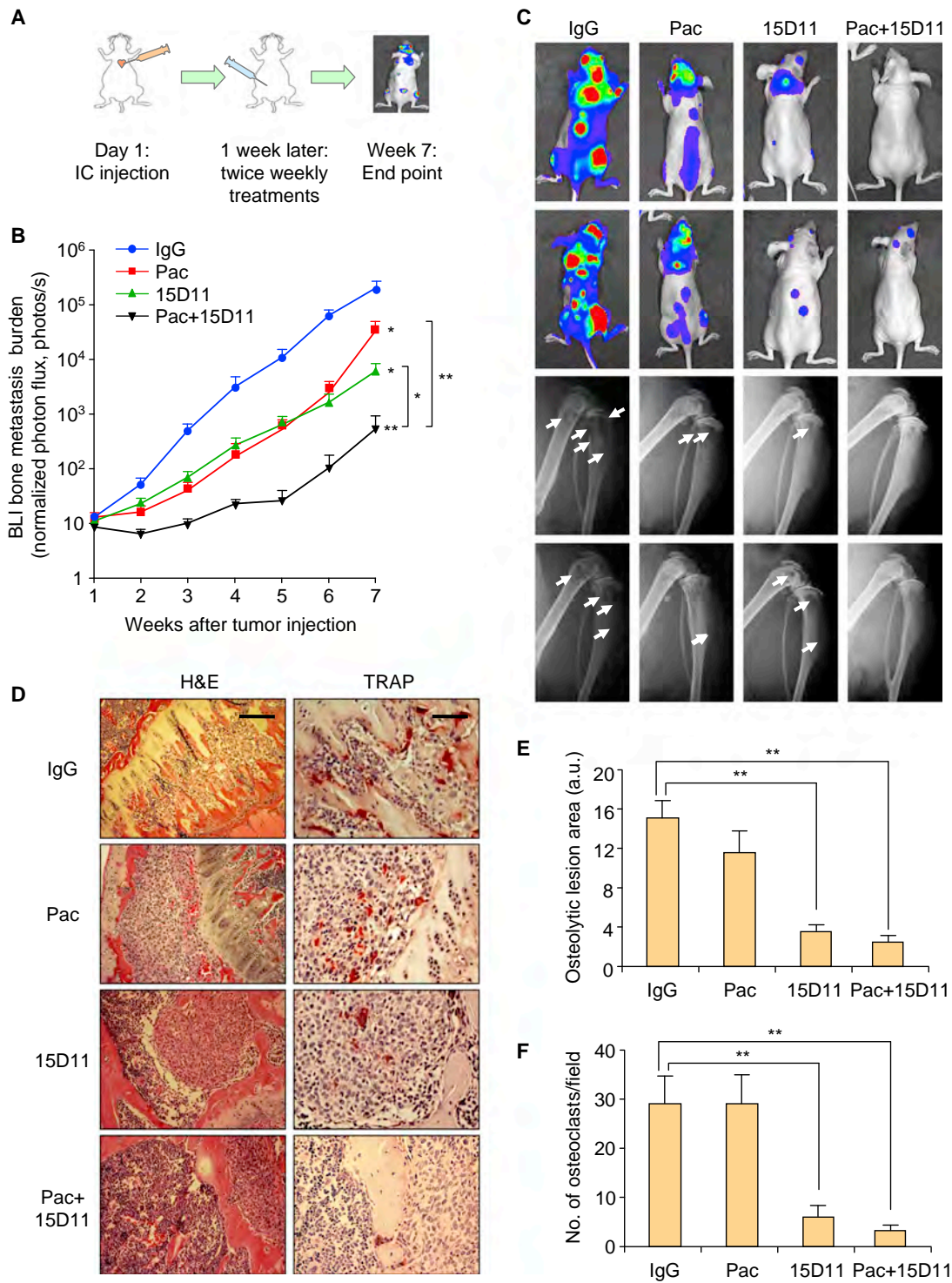
Figure 3. Synergistic Inhibition of SCP28-Jagged1 Bone Metastasis with Combined Treatment of 15D11 and Chemotherapy

(A) Schematic representation of the experiment. 10^5 tumor cells were IC injected into each mouse. Treatments were initiated 1 week after the injection and continued twice a week at the dosage of 10 mg/kg for IgG/15D11 and 20 mg/kg for paclitaxel.

(B) Quantification of bone metastasis burden each week based on BLI imaging. n = 10 mice per group; data presented as mean ± SEM. *p < 0.05 and **p < 0.01 by Mann-Whitney test.

(C) Representative BLI and X-ray images of two mice per group at week 7. Arrows indicate osteolytic bone areas.

(legend continued on next page)

the preventive treatment protocol, 15D11 treatment reduced the number of osteoclasts and decreased osteolytic bone areas, although some basal level of osteoclasts can still be observed, compared with the near complete absence of osteoclasts in mice treated with OPG-Fc (Figures S2E–S2G).

Jagged1 has been extensively studied for its role in developmental angiogenesis (Benedito et al., 2009). Therefore, we tested the inhibitory effect of 15D11 on angiogenesis using two different angiogenesis models. In both neonatal mouse retina and subcutaneous xenograft tumor angiogenesis assays (Polverino et al., 2006; Ridgway et al., 2006), 15D11 treatment showed no effect on angiogenesis (Figures S3A–S3D). Therefore, it is unlikely that 15D11 reduces bone metastasis through inhibiting angiogenesis.

15D11 Sensitizes Bone Metastases to Chemotherapy

Chemotherapy is commonly used to manage bone metastasis, although bone lesions are usually more refractory to chemotherapy (Gu et al., 2004). To evaluate the combinatorial effect of 15D11 with conventional chemotherapy, we treated bone metastasis generated by SCP28-Jagged1 cells with 15D11 and paclitaxel, using the late treatment protocol (treatment initiated 1 week after IC injection) (Figure 3A). The mouse group injected with SCP28-Jagged1 progressed slowly to the moribund state compared with the mouse group injected with SCP2 (7 weeks compared with 4 weeks with SCP2), which provided us with a sufficient time to observe the therapeutic effect of single or combinatory treatment of 15D11 and paclitaxel. Mice were treated with IgG, 15D11, paclitaxel, or both 15D11 and paclitaxel, 1 week after IC injection of SCP28-Jagged1 to establish bone metastases. Monotherapy using 15D11 resulted in a nearly 10-fold reduction of metastasis burden (Figure 3B). While paclitaxel alone significantly slowed down bone metastasis progression at early time points, resistance to chemotherapy emerged at later time points, resulting in only a mild reduction of tumor burden at the endpoint of the experiment (Figure 3B). Strikingly, when mice were treated with both 15D11 and paclitaxel, a synergistic >100-fold reduction of bone metastasis was observed compared with the IgG control group (Figures 3B and 3C). X-ray images and TRAP staining for osteoclasts confirmed significant decrease of osteoclast number and osteolytic lesions after 15D11 treatment alone or combined with chemotherapy (Figures 3C–3F). In particular, there is almost no osteolytic bone area in the combined treatment group, consistent with the BLI data. Taken together, these results demonstrate a potent synergistic effect of combined treatment of paclitaxel and 15D11 in diminishing bone metastasis generated by SCP28-Jagged1.

This strong inhibitory effect of the combined treatment on bone metastasis could potentially be explained by the combined effect of blocking Jagged1-dependent stromal engagement by 15D11 and cytotoxicity of paclitaxel to tumor cells. If this is indeed the case, no synergistic therapeutic benefit should be expected when chemotherapy is combined with 15D11 for the treatment of bone metastasis generated by tumor cells with

low or no Jagged1 expression. We thus used the parental SCP28 cells, which has very low endogenous Jagged1 level (Figure S4A), to test this directly. We performed the same bone metastasis and treatment experiments as we did with SCP28-Jagged1 (Figure 4A). Paclitaxel initially reduced bone metastasis burden, but the lesions quickly become refractory to chemotherapy and only slightly reduced metastatic burden (Figures 4B and 4C). As expected from the lack of Jagged1 expression in SCP28, 15D11 had no effect on reducing bone metastasis burden by SCP28 (Figures 4B and 4C). To our surprise, the combined treatment group displayed a dramatic reduction of bone metastasis burden, decreased osteolytic bone lesion areas, and reduced osteoclast number (Figures 4B–4F). Such a therapeutic response is far superior than single treatment of either paclitaxel or 15D11 alone, suggesting a synergy of targeting Jagged1 along with chemotherapy for bone metastasis, even in tumor cells with low levels of Jagged1 expression.

To validate whether the observed synergy of combined treatment can also be observed in other models of bone metastasis beyond the MDA-MB-231 series, we used the bone metastatic SUM1315-M1B1 cell line, which has been recently developed in our laboratory by in vivo selection for increased bone metastatic propensity (our unpublished data) from the parental SUM1315 breast cancer cell line (Forozan et al., 1999). SUM1315-M1B1 has a similarly low basal level of Jagged1 expression as SCP28 (Figure S4A). Again, a significant reduction of bone metastasis burden, osteolytic lesion area, and osteoclast numbers was only observed in mice treated with both paclitaxel and 15D11 (Figures S4B–S4G). Taken together, we identified a potent synergistic inhibitory effect on bone metastasis by combining chemotherapy and 15D11, and such therapeutic synergy is not dependent on high expression level of Jagged1 in tumor cells.

Chemotherapy Induces Jagged1 Expression in Osteoblast Lineage Cells

We considered the possibility that chemotherapy agents may induce Jagged1 expression in either tumor cells or in the bone stromal cells. Such chemotherapy-induced Jagged1 might contribute to the resistance of bone metastasis to chemotherapy and can be targeted by 15D11, as we saw in the combined treatment. Key stromal cell types in bone metastasis include osteoclasts, osteoblasts and their progenitors (such as MSCs), and endothelial cells. We tested if Jagged1 could be induced in these cells and various breast cancer cell lines upon treatment of two different chemotherapy agents, paclitaxel and cisplatin, which are commonly used in the treatment of breast cancer. Jagged1 expression was significantly increased only in MC3T3-E1 pre-osteoblast cell and MSCs (Ren et al., 2008) (Figure 5A). There was no significant induction of Jagged1 in endothelial cells, RAW 264.7 pre-osteoclasts, or in SCP28 and SUM1315-M1B1 tumor cells (Figure 5A).

To confirm this finding in vivo, female nude mice were treated with either PBS or cisplatin. Hindlimb bones were dissected

---

(D) Representative H&E and TRAP staining images from the experiment at the endpoint. Scale bars, 100 μm for H&E and 50 μm for TRAP.

(E) Quantification of osteolytic lesions based on X-ray images from (D), n = 10 mice per group; data presented mean ± SEM. **p < 0.01 by Student's t test.

(F) Quantification of TRAP$^+$ osteoclasts from decalcified histological bone sections of hindlimbs from mice in (D), n = 10 per group. Data are presented as mean ± SEM. **p < 0.01 by Student's t test.
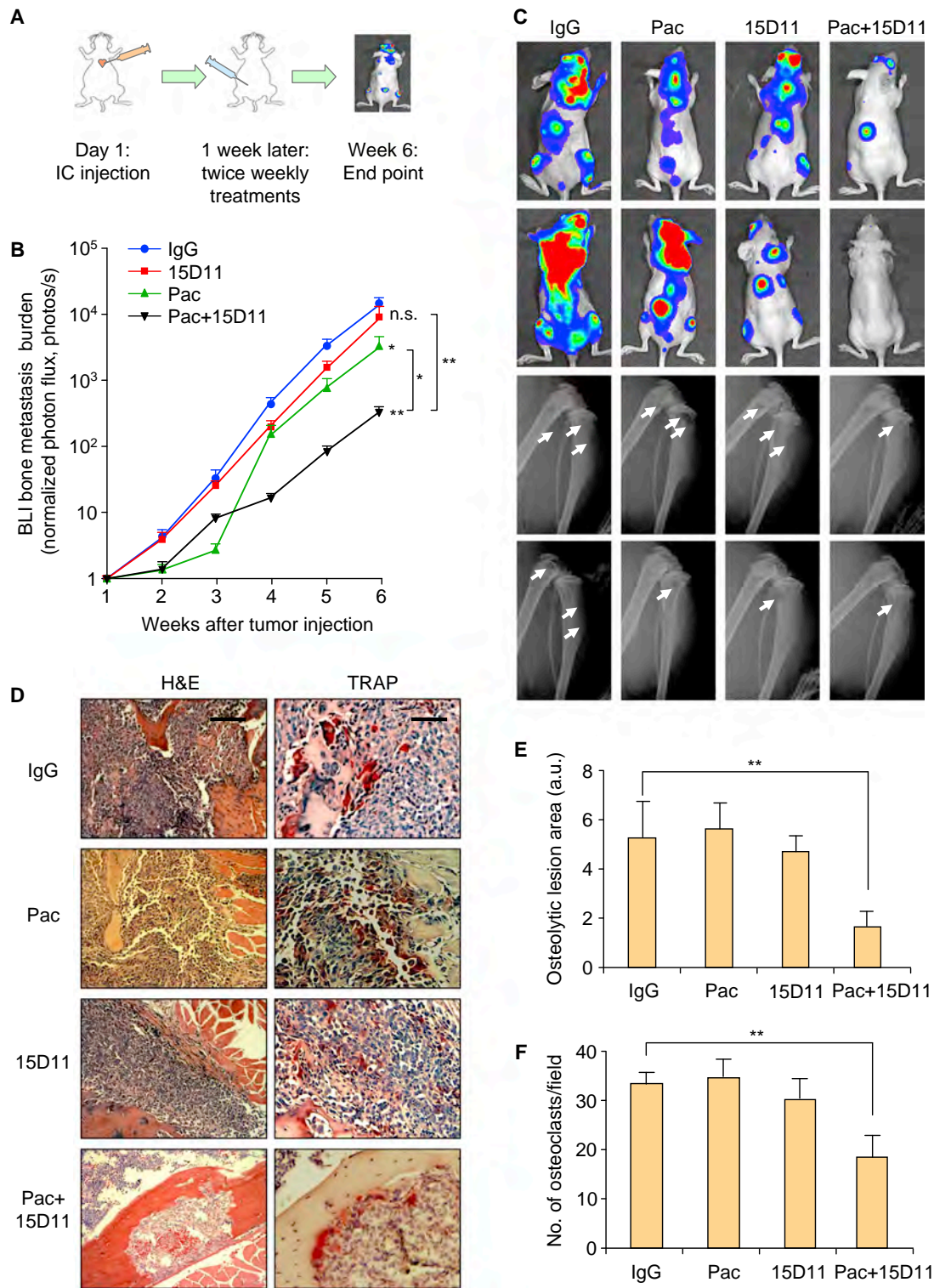
Figure 4. Synergistic Inhibition of SCP28 Bone Metastasis with Combined Treatment of 15D11 and Chemotherapy

(A) Schematic illustration of the experimental procedure. 10^5 tumor cells were IC injected into each mouse. Treatments were initiated 1 week after the injection and continued twice a week at the dosage of 10 mg/kg for IgG/15D11 and 20 mg/kg for paclitaxel.

(B) Quantification of bone metastasis burden based on BLI imaging. n = 10 mice per group; data presented as mean ± SEM. *p < 0.05 and **p < 0.01 by Mann-Whitney test.

(C) Representative BLI images and X-ray images at week 6 of two mice per group. Arrows indicate osteolytic bone areas.

(legend continued on next page)

48 hr later and immuno-stained with antibodies against Jagged1 and alkaline phosphatase (ALP), a marker for osteoblast cells. In the PBS control group, Jagged1+ cells were rarely detected and mostly co-localized with ALP+ osteoblasts. Cisplatin treatment induced much stronger Jagged1 expression based on immuno-staining analysis, and these Jagged1+ cells again mostly over-lapped with ALP+ cells (Figure 5B). This result thus indicates that chemotherapy induces Jagged1 expression in osteoblast cells *in vivo*.

We next sought to understand which signaling pathway is responsible for Jagged1 induction after chemotherapy in osteo-blast lineage cells. Chemotherapy generates many stress re-sponses in cells, including endoplasmic reticulum (ER) stress and oxidative stress. Some of the stress conditions have been associated with the regulation of Jagged1 expression (Paul et al., 2014). We utilized several treatments to mimic or inhibit these stress responses and then analyzed Jagged1 mRNA and protein levels within the cells. Among these treatments, we de-tected that ascorbate, which induces oxidative stress when used at high concentration, and H_2O_2 induced strong Jagged1 expression in MSCs, while ER stress inducers Brefeldin A and Tunicamycin did not induce Jagged1 expression (Figures S5A and S5B). Consistent with this observation, cisplatin and doce-taxel induced reactive oxygen species (ROS) production in MSCs, which could be completely blocked by N-acetyl cysteine (NAC), an ROS inhibitor (Figure S5C). Administration of NAC also completely blocked cisplatin-induced Jagged1 expression in MSCs (Figure S5D). These results indicate that Jagged1 is induced in osteoblastic lineage cells during chemotherapy, likely through the ROS pathway.

Osteoblast-Derived Jagged1 Promotes Bone Metastatic Seeding and Chemoresistance

To directly test the effect of increased Jagged1 expression in os-teoblasts on bone metastasis seeding and progression, we uti-lized two models. In the first model, athymic nude mice were either treated with PBS or cisplatin, which has a much shorter half-life than paclitaxel. One day later, we inoculated tumor cells to the hindlimbs using the intra-iliac artery (IIA) injection method (Wang et al., 2015) to specifically study the stromal effect on bone metastasis seeding after chemotherapy, as tumor cells were not exposed to a clinical dose of cisplatin in this experi-mental setting. In all three different cancer cell lines tested (MCF7, SCP28, and SUM1315-M1B1), there was a significant in-crease of bone metastatic seeding (Figures 5C–5E). Immuno-staining confirmed that there were significantly more GFP+ tumor cells in the bone among mice pre-treated with cisplatin, and these tumor cells are usually located in close proximity to ALP+ osteoblasts (Figure 5F; Movies S5 and S6).

Since chemotherapy may have broad systemic effects on mice that may directly or indirectly influence the outcome of the experiment that we described above, we decided to use an alternative approach to specifically increase Jagged1 expres-sion in osteoblasts without using chemotherapy. To this end,

we generated a transgenic mouse strain with osteoblast-specific Jagged1 overexpression driven by the Col1a1 promoter (Figures S6A and S6B). The Col1a1-Jag1 mice are generally healthy and fertile (our unpublished data), but developed a significant short-ening and swelling of bone in the middle region of both femur and tibia (Figure S6C). μCT imaging and bone histology analysis showed decreased bone density and highly trabecularized bone in the cortical bone area, there was also significant decrease of bone density in trabecular bone region (Figure 6A and data not shown). We also found excessive TRAP+ osteo-clasts in the cortical bone of Col1a1-Jag1 mice (Figure 6B), consistent with the previously reported function of Jagged1 in promoting osteoclastogenesis (Sethi et al., 2011). After Col1a1-Jag1 mice were treated with 15D11 for 3 months, exces-sive TRAP+ osteoclasts in Col1a1-Jag1 mice were reduced significantly, confirming that the phenotype in this mouse strain is indeed caused by osteoblast-derived Jagged1 (Figure 6B).

Next, we tested the long-term bone metastasis progression and short-term metastatic seeding on these mice. For the long-term bone metastasis assay, we used the syngeneic PyMT-A-FIG cell line previously established in our lab from an MMTV-PyMT mammary tumor (Wan et al., 2014) and stably labeled with the Firefly-IRES-GFP (FIG) reporter to facilitate *in vivo* tracking. PyMT-A-FIG cells were inoculated to wild-type (WT) or Col1a1-Jag1 mice via intra-tibial injection to generate bone metastasis. BLI analysis showed a nearly 20-fold increase of bone metastasis tumor burden in Col1a1-Jag1 mice than that in WT mice (Figure 6C). To test the short-term bone metastasis seeding, we injected PyMT-A-FIG cells by IIA into either Col1a1-Jag1 mice or WT mice. Four days after tumor inocula-tion, there were already ∼3 times more tumor cells surviving in the bone of Col1a1-Jag1 mice than in WT mice (Figure 6D). Im-munostaining revealed more seeding of GFP+ tumor cells in bone of Col1a1-Jag1 mice, often in close contact with ALP+ osteo-blasts (Figure 6E). Taken together, these results confirmed that osteoblast-derived Jagged1 promotes bone metastatic seeding and outgrowth.

To mimic chemoresistance and tumor seeding effects by oste-oblast lineage cells *in vitro*, we adapted an *in vitro* 3D tumor-stroma co-culture assay (Wang et al., 2015). Consistent with the previous report, when tumor cells were co-cultured with osteoblast lineage cells in low attachment plates, they generated heterotypic spheres, with tumor cells forming an outside shell-like structure and osteogenic cells forming an inner core sphere (Figure S7A). There was increased survival of co-cultured tumor spheres compared with tumor-only spheres when treated with cisplatin or docetaxel (a potent form of paclitaxel) (Figure 7A), suggesting that osteoblast lineage cells promote the survival of tumor cells during chemotherapy. To examine cellular apoptotic pathway status, cell lysates were collected from either SCP28 culture alone or in co-culture with MC3T3 cells. Seventy-two hours post-treatment of cisplatin, there was a strong induc-tion of cleaved PARP and cleaved caspase-3 (CC3) CC3 in SCP28 singe-cultured cells, while the level of these apoptotic

(D) Representative H&E and TRAP staining images from the experiment at the endpoint. Scale bars, 100 μm for H&E and 50 μm for TRAP.
(E) Quantification of osteolytic lesions based on X-ray images from (D). n = 10 mice per group. Data are presented as mean ± SEM. **p < 0.01 by Student's t test.
(F) Quantification of TRAP+ osteoclasts from decalcified histological bone sections of hindlimbs from mice in (D), n = 10 per group; data presented as mean ± SEM. **p < 0.01 by Student's t test. See also Figure S4.
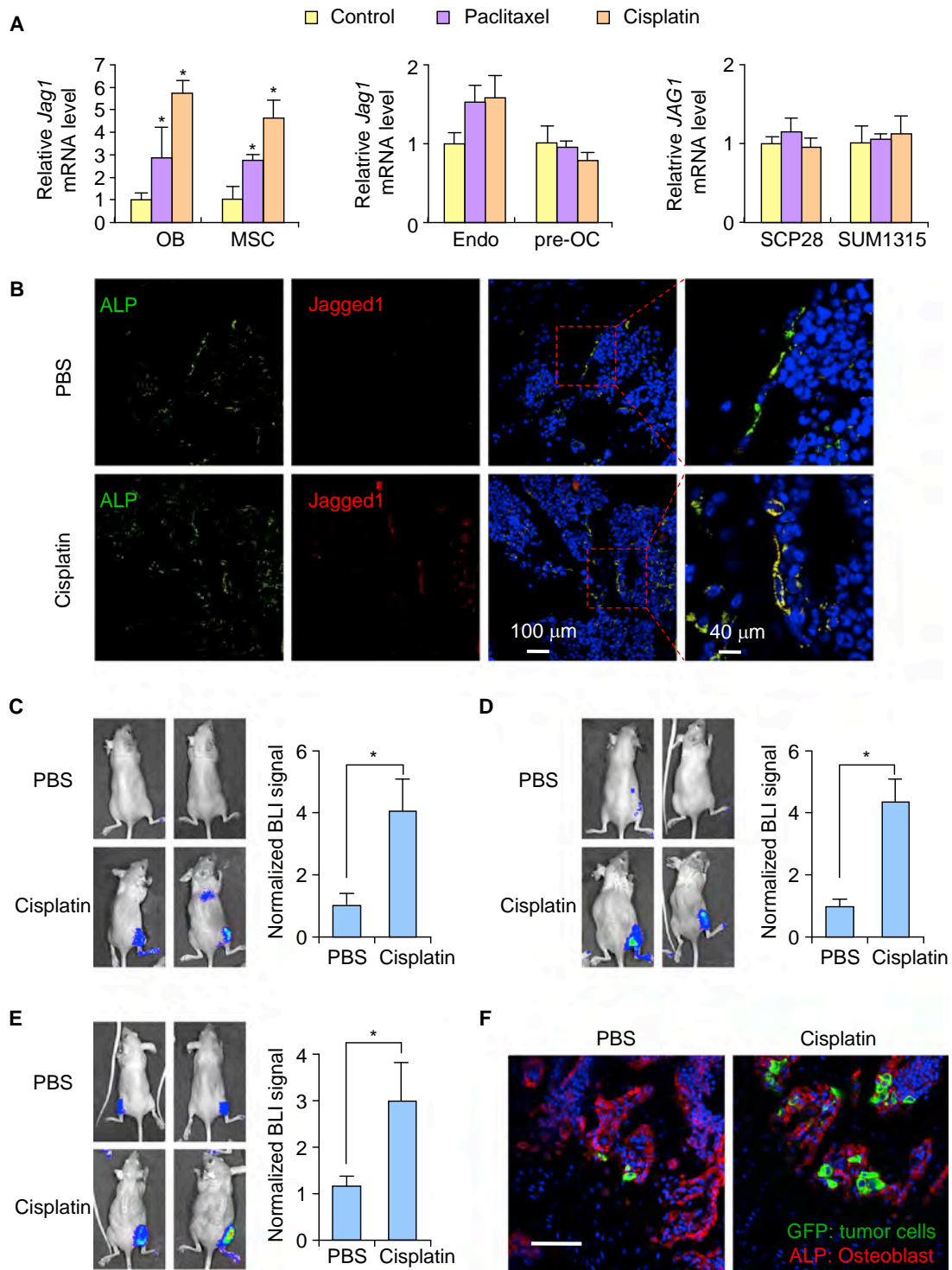
Figure 5. Chemotherapy Induces Jagged1 Expression in Osteoblast Lineage Cells

(A) Jagged1 mRNA expression in osteoblast (OB) MC3T3-E1 clone no. 4 osteoblast cells and mesenchymal stem cells (MSC), HPMECL endothelial cells (endo), RAW264.7 pre-osteoclasts (pre-OC), and SCP28 and SUM1315-M1B1 breast tumor cells 48 hr post-treatment with 25 nM paclitaxel or 10 μM cisplatin. n = 3 per group; data presented as mean ± SEM. *p < 0.05 by Student's t test.

(B) Athymic nude mice were intravenously (i.v.) injected with PBS or cisplatin (2 mg/kg) and euthanized 48 hr later. Hindlimb bones were collected for IF staining against ALP (green) and Jagged1 (red). Nuclei were counter-stained with DAPI (blue).

(legend continued on next page)

pathway-related proteins was still at low levels in co-culture samples (Figure 7B). To determine whether direct cell-cell contact is needed for the observed chemoresistance, we collected conditioned medium (CM) from cisplatin-treated MSCs and performed the same assay. We found tumor cells were only partially protected from chemotherapy in the presence of CM compared with higher resistance to chemotherapy of tumor cells co-cultured with MSCs (Figure S7B). This result indicates that the direct tumor-stromal cell contact, which is required for Notch signaling, is needed for optimal Jagged1-mediated chemoresistance. Indeed, when we analyzed Notch downstream gene expression in co-cultured tumor cells after either cisplatin or docetaxel treatment, we found multiple Notch downstream genes, including human *HES2*, *HEY1*, and *HEY2*, were significantly upregulated in co-culture tumors cells after chemotherapy (Figure 7C). Co-culture of tumor cells with endothelial cells provided no protective effect during cisplatin or docetaxel treatment (Figures S7C and S7D), suggesting that only osteoblast lineage cells, but not endothelial cells, protect tumor cells against chemotherapy in the bone.

Notch activation is reported to circumvent apoptosis through affecting the p53-regulated apoptotic pathway (Dotto, 2009). We compared gene expression profile of SUM1315-M1B1 tumor cells before and after cisplatin treatment, in the presence or absence of osteoblast co-culture. We focused our analysis on 161 apoptosis-related genes (see the STAR Methods for details). Among apoptosis-related genes that have more than 2-fold differential expression in co-culture versus tumor culture alone in cisplatin treatment conditions, ten are anti-apoptotic genes that were reduced in expression upon cisplatin treatment in tumor culture alone, but were elevated in basal expression levels and further increased upon cisplatin treatment in the co-culture condition. Similarly, six pro-apoptotic genes were induced in tumor cells alone by cisplatin treatment, but such change was suppressed in the co-culture condition (Figure 7D). Notably, among those 16 genes, at least 5 genes are known to be regulated by the p53 pathway. *MCL1, CCNA1, GADD45*, and *BAX* are direct transcriptional targets of p53 and *CCND2* is an indirect p53 pathway gene. Taken together, these results suggested that osteoblast-mediated chemoresistance of tumor cells is at least in part mediated by Notch activation and its effect on suppressing p53-regulated apoptotic pathway.

To directly analyze whether Jagged1 protects tumor cells from chemotherapy-induced apoptosis, we performed immunofluorescent staining of GFP+ tumor cells and CC3 of mouse bone sections after two rounds of single or combined treatments of paclitaxel and 15D11, as in the experiment in Figure 4A. There was almost no detectable CC3 staining in either the IgG- or the 15D11-treated group,. While a substantial number of tumor cells in the paclitaxel treatment group were positive for CC3, the paclitaxel and 15D11 combinational treatment group had the highest abundance of CC3+ tumor cells (Figures 7E and 7F).

To test whether Jagged1 antibody 15D11 could block the survival benefits conferred by MSCs during chemotherapy, we co-cultured SCP28 and SUM1315-M1B1 cells with MSCs. At the time of treating cells with chemotherapy, cells were also incubated with IgG or 15D11 antibody. Administration of 15D11 significantly reduced the number of surviving tumor spheres when the tumor cells were co-cultured with MSCs (Figures S7E and S7F). Similar findings were observed in co-culture experiment with MC3T3 cells. To confirm this result *in vivo*, we treated nude mice with cisplatin 1 day before the tumor cell injection. Right at the time of IIA injection of SUM1315-M1B1 tumor cells, mice were also treated with either IgG or 15D11 antibody. Bone metastatic seeding was tracked by BLI and by immunofluorescence (IF) staining 4 days after the injection. Similar to the earlier experiment (Figures 5C–5E), more tumor cells were seeded in the bone of the mice pre-treated with cisplatin (Figure 7G). Such an increase of metastatic seeding in chemotherapy-primed bone was largely eliminated by 15D11 treatment. Similar result was also obtained using ER+ MCF7 breast cancer cells (Figures S7G and S7H). Confocal IF imaging of bone sections from euthanized animals further confirmed increased seeding of tumor cells next to ALP+ osteoblasts in chemotherapy-primed mice and the subsequent decrease after treatment with 15D11 (Figure 7H). In conclusion, our results demonstrate that, although chemotherapy is cytotoxic to tumor cells, its full therapeutic potential is compromised by the increased expression of Jagged1 in osteoblast lineage cells in response to chemotherapy. Osteoblast-derived Jagged1 activates Notch signaling in tumor cells to promote resistance to chemotherapy-induced apoptosis. Combining chemotherapy with 15D11 treatment will nullify such stroma-mediated mechanism of chemoresistance, and achieve optimal outcome in the treatment of bone metastasis.

Combinatorial Treatment of 15D11 and Chemotherapy Synergistically Reduces the Incidence of Spontaneous Bone Metastasis

Our mouse model study revealed a role of chemotherapy-induced Jagged1 in osteoblasts in promoting chemoresistance of bone metastasis. To confirm whether Jagged1 is also induced in osteoblasts in human cancer patients receiving chemotherapy, we acquired the paired bone marrow cytospin samples of patients before and after receiving the adjuvant chemotherapy of carboplatin and paclitaxel and performed immunostaining analysis. Prior to chemotherapy, Jagged1 was expressed at a low level, mostly on ALP+ osteoblasts (Figure 8A). After chemotherapy, there is a significant increase of Jagged1 staining on osteoblasts (Figures 8A and 8B), consistent with our observation from *in vitro* and mouse models (Figures 5A and 5B).

In the clinical management of early-stage breast cancer, neoadjuvant and adjuvant chemotherapy is commonly used to prevent future relapse. Although chemotherapy certainly decreases the local relapse and bone metastasis, it is potentially diminished

(C–E) Athymic nude mice were treated with either PBS or cisplatin (2 mg/kg) on day 0. One day after the pre-treatment, MCF7 (C), SUM1315-M1B1 (D), or SCP28 (E) cells were delivered locally to the hindlimbs of these mice by IIA injection. BLI imaging and quantification of BLI signal at day 4. n = 5; data presented as mean ± SEM. *p < 0.05 by Student's t test.

(F) Mice from experiment in (E) were euthanized after BLI imaging at day 4. Hindlimbs were fixed and processed for IF imaging of GFP-expressing tumor cells (green) and ALP+ osteoblasts (red). Scale bar, 80 μm. See also Figure S5 and Movies S5 and S6.
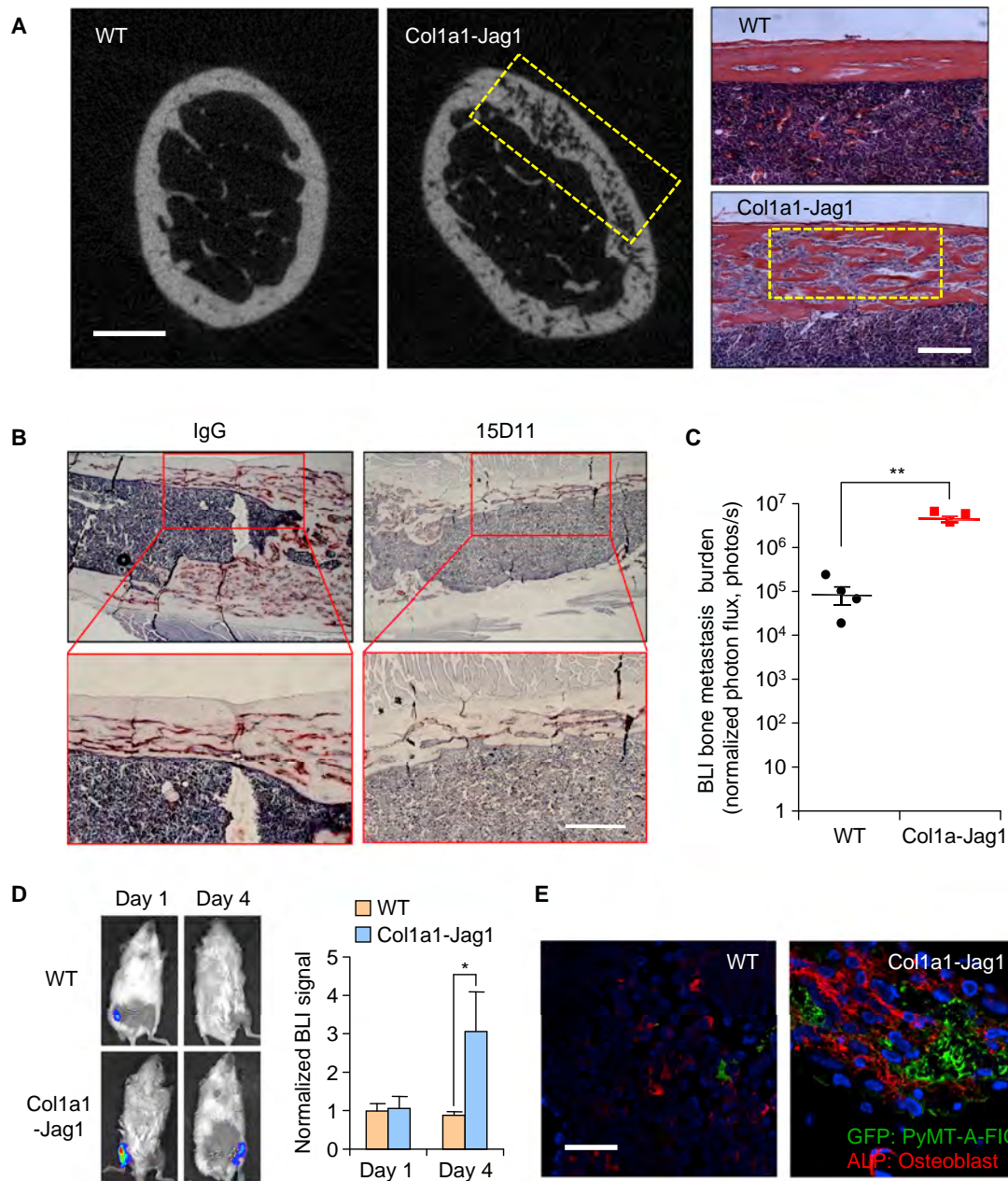
Figure 6. Osteoblast-Derived Jagged1 Promotes Bone Metastasis Seeding and Progression

(A) Representative µCT imaging and H&E staining images from FVB WT and Col1a1-Jag1 mice. Yellow box: trabecular bone areas of decreased bone density (in µCT imaging) that were filled with bone marrow cells (in H&E staining). Scale bars, 0.5 mm in µCT and 200 µm in H&E.

(B) Col1a1-Jag1 mice were treated with IgG or 15D11 (10 mg/kg) twice a week for 3 months. Mice were then euthanized for bone sample collection and histology analysis. Representative TRAP staining images from IgG or 15D11 group were presented. Scale bar, 200 µm.

(C) PyMT-A-FIG cells were delivered locally to the hindlimbs of WT and Col1a1-Jag1 mice by intra-tibial injection. Three weeks after injection, the engraftment of breast cancer cells in the bone was assessed by BLI. Each data point represents an individual mouse (n = 4); horizontal line represents mean ± SEM. **p < 0.01 by Student's t test.

(D) PyMT-A-FIG cells were delivered locally to the hindlimbs of WT and Col1a1-Jag1 mice by IIA injection. Tumor cells in the bone were quantified based on BLI imaging at day 1 and day 4 (right panel). n = 5; data presented mean ± SEM. *p < 0.05 by Student's t test.

(E) IF staining of bone samples at day 4 from experiment in (C), showing GFP-expressing tumor cells (green) and ALP⁺ osteoblasts (red). Scale bar, 80 µm. See also Figure S6.

by the chemotherapy-induced osteoblast Jagged1 in promoting metastatic seeding in bone. Therefore, combining chemotherapy and 15D11 treatment may further decrease the risk of

bone relapse. To test this notion, we utilized 4T1.2 mammary tumor cells, which can spontaneously metastasize to the bone from the mammary glands (Eckhardt et al., 2005). 4T1.2 tumor
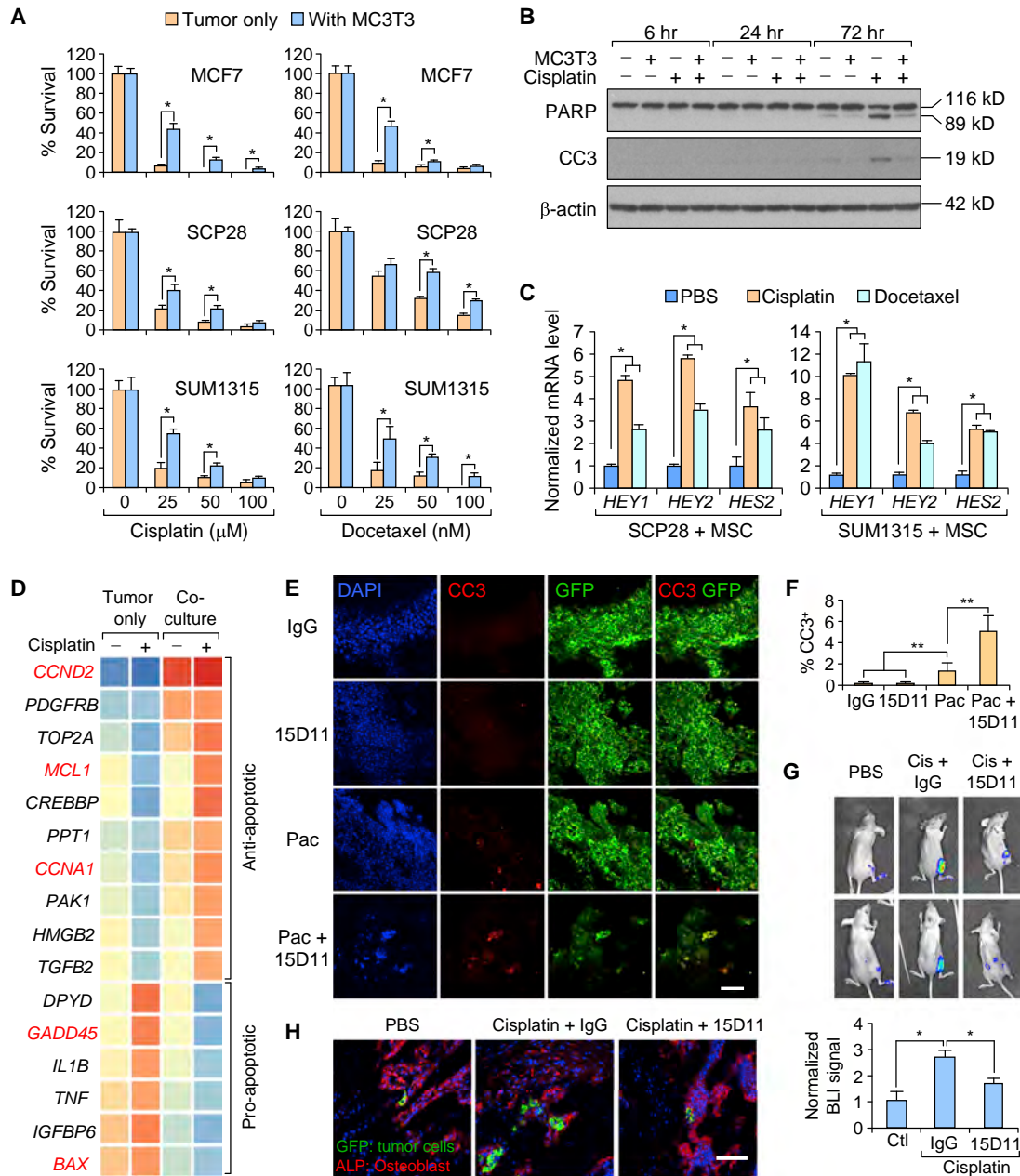
Figure 7. Pro-survival Effect of Osteoblast Jagged1 on Cancer Cells Can Be Blocked by 15D11

(A) 3D tumor sphere culture of MCF7, SCP28, and SUM1315-M1B1 cells, alone or in co-culture with osteoblast cells, were treated with indicated concentrations of cisplatin or docetaxel. Two days after the chemotherapy, the surviving tumor spheres were counted under the fluorescent microscope. n = 3 per group; data presented as mean ± SEM. *p < 0.05 by Student's t test.

(B) Cell culture of SCP28 cells alone or in co-culture with MC3T3-E1 pre-osteoblast cells were treated with PBS or cisplatin. Protein samples were collected 6, 24, and 72 hr later. Cleaved PARP and cleaved caspase-3 were determined by immunoblotting. Full-length PARP is 116 kDa and cleaved PARP is 89 kDa.

(C) Real-time PCR analysis of Notch target genes (*HEY1*, *HEY2*, and *HES2*) in tumor cells co-cultured with MSC and treated with indicated chemotherapeutic agents. n = 3 per group; data presented as mean ± SEM. *p < 0.05 by Student's t test.

(D) Microarray analysis was performed with mRNA from cell culture of SUM1315-M1B1cells alone or in co-culture with MC3T3-E1 osteoblasts, with or without cisplatin treatment. Heatmap shows 16 apoptosis-related genes with at least 2-fold change in the cisplatin treatment condition (tumor cell culture alone versus co-culture). Five p53 pathway-related genes were highlighted in red.

(E and F) 10^5 SCP28 cells were IC injected into each mouse. Treatments were initiated 1 week after the injection for twice at the dosage of 10 mg/kg for IgG/15D11, and 20 mg/kg for paclitaxel. Hindlimb bones were collected, fixed and cryo-sectioned for IF staining against CC3 for apoptotic cells and GFP for tumor cells (E), and CC3$^+$ apoptotic cells among GFP$^+$ tumor cells were quantified in (F). Scale bar, 25 μm. n = 5 mice per group; data presented as mean ± SEM. **p < 0.01 by Student's t test.

(legend continued on next page)

cells were injected into mammary fat pads of female BALB/c mice to allow the establishment of primary tumors. Once the primary tumor sizes reached 5 mm, mice were randomly grouped for treatment with IgG, paclitaxel, 15D11, or both paclitaxel and 15D11 (Figure 8C). Based on X-ray images, we noticed that over 50% of mice in the IgG control group developed bone metastasis in their hindlimb bones. 15D11 or paclitaxel treatment reduced bone metastasis incidence by 15%–30%, while a strong inhibition of bone metastasis was achieved by paclitaxel and 15D11 combinatorial treatment, with only 10% of mice developing bone metastasis (Figures 8D and 8E). Bone lesion areas were also significantly reduced in combinational treatment (Figure 8F). Overall, these results suggest that treating cancer patients with adjuvant chemotherapy combined with 15D11 could potentially reduce the incidence of future bone metastasis relapse.

DISCUSSION

As one of the major ligands for Notch, Jagged1 has been recently shown to be an important driver of cancer progression, including metastasis to bone (Sethi et al., 2011). In our effort to develop therapeutic antibodies against Jagged1, we utilized the XenoMouse technology to develop fully human Jagged1 antibodies and selected 15D11 for further testing based on blocking efficacy, affinity, and specificity. 15D11 displayed no detectable side effects in vivo, while retaining a robust ability to inhibit Jagged1-mediated signaling in vitro, and reduced in vivo bone metastasis of Jagged1-expressing breast cancer cells. In contrast to OPG-Fc, a decoy receptor for RANKL, 15D11 only inhibits pathological osteoclastogenesis, but maintains a basal number of osteoclasts, which is required for normal bone homeostasis, avoiding the abnormal increase of bone density typically observed after OPG-Fc, denosumab, or bisphosphonate treatments. Thus, 15D11 represents a promising candidate for further clinical development as a therapeutic agent for bone metastasis.

While chemotherapy is effective in controlling or even curing different types of cancer, development of chemoresistance, especially in metastatic cancer, often leads to eventual mortality from cancer (Anampa et al., 2015). Understanding the mechanism of chemoresistance is crucial for developing strategies to re-sensitize chemo-resistant tumors. Previous studies of chemoresistance have mostly focused on tumor-intrinsic mechanisms, such as reduced drug uptake or increased drug efflux, alterations in drug-target interaction, changes in cellular response, in particular increased cell ability to repair DNA damage or tolerate stress conditions, and defects in apoptotic pathways. However, the tumor microenvironment, especially the unique stromal niches in the organ sites of metastasis, may also have a major influence on the development of chemoresistance. In our current study, we uncovered a tumor-osteoblast interaction that promotes chemoresistance of bone metastasis. Here we demonstrate that various chemotherapy agents, including paclitaxel and cisplatin, induced Jagged1 expression in osteoblasts and MSCs, which feeds back to tumor cells to activate Notch signaling and promote chemoresistance. Administration of 15D11 into our in vitro 3D co-culture system or in various mouse models of bone metastasis significantly increased the sensitivity of tumor cells and bone metastasis to chemotherapy. Most strikingly, when chemotherapy was combined with 15D11, a nearly 100-fold reduction of bone metastasis burden was observed in our mouse model of bone metastasis. Thus, 15D11 represents a unique therapeutic agent capable of targeting both tumor-derived Jagged1 and chemotherapy-induced Jagged1 in osteoblasts, thus inhibiting multiple downstream Notch signaling events that are important for both the expansion of osteolytic lesions and chemoresistance of cancer cells in bone (Figure 8G).

Jagged1 is overexpressed in a proportion of primary breast tumors and these tumors are prone to develop bone metastasis (Li et al., 2014; Sethi et al., 2011). However, Jagged1 expression in tumor cells is not able to induce their own Notch signaling activation (Sethi et al., 2011). In our current study, Notch signaling is activated in tumor cells only when they are interacting with osteoblast Jagged1 during chemotherapy. This observation is consistent with the known Notch trans-activation and cis-inhibition mechanism. For example, during the development of Drosophila eyes, although adjacent cells express both Notch ligands and receptors, the Notch signaling activation only occurs in one direction, but not in both cells, setting up the developmental pattern within the tissue (Miller et al., 2009). More importantly, Notch ligands also generate cis-inhibitory signals on the same cell (Sprinzak et al., 2010). Future studies should explore the exact reason why tumor-derived Jagged1 is not able to induce its own Notch activation, and how chemotherapy and oxidative stress specifically induce Jagged1 in osteoblast lineage cells but not in tumor cells and other stromal cells. It is also possible that additional stromal cell types, including the vascular endothelial cells, osteoclast cells, neurons, and bone marrow cells may also contribute to therapy resistance through different molecular mechanisms (Duan et al., 2014; Hanoun et al., 2014; Pitt et al., 2015), which would be an interesting direction for further investigations.

After resection of the primary tumor, many breast cancer patients are treated with adjuvant chemotherapy to reduce the risk of future relapse. Despite the proven therapeutic benefit of adjuvant chemotherapy in reducing relapse, a substantial portion of breast cancer patients eventually still develop metastatic relapse in bone and other organs (Anampa et al., 2015). Indeed, DTCs are frequently observed in breast cancer patients long after the surgical removal of the primary tumors and adjuvant chemotherapy, and the presence of these DTCs correlates with risk of metastatic relapse (Braun et al., 2005). These findings

(G) Athymic nude mice were treated with either PBS or cisplatin via i.v. injection on day 0. On day 1, PBS pre-treated mice were treated with IgG, while cisplatin pre-treated mice were treated with either IgG or 15D11. SUM1315-M1B1 cells were delivered locally to the hindlimbs of these nude mice by IIA injection. Tumor cells in the bone were quantified based on BLI imaging on day 1 and day 4. BLI signal at day 4 was normalized to BLI signal intensity at day 1 (lower panel). n = 5; data presented as mean ± SEM. *p < 0.05 by Student's t test.

(H) Mice from experiment in (G) were euthanized after BLI imaging at day 4. Hindlimbs were fixed and processed for IF imaging of GFP-expressing tumor cells (green) and ALP[+] osteoblasts (red). Scale bar, 40 μm. See also Figure S7.
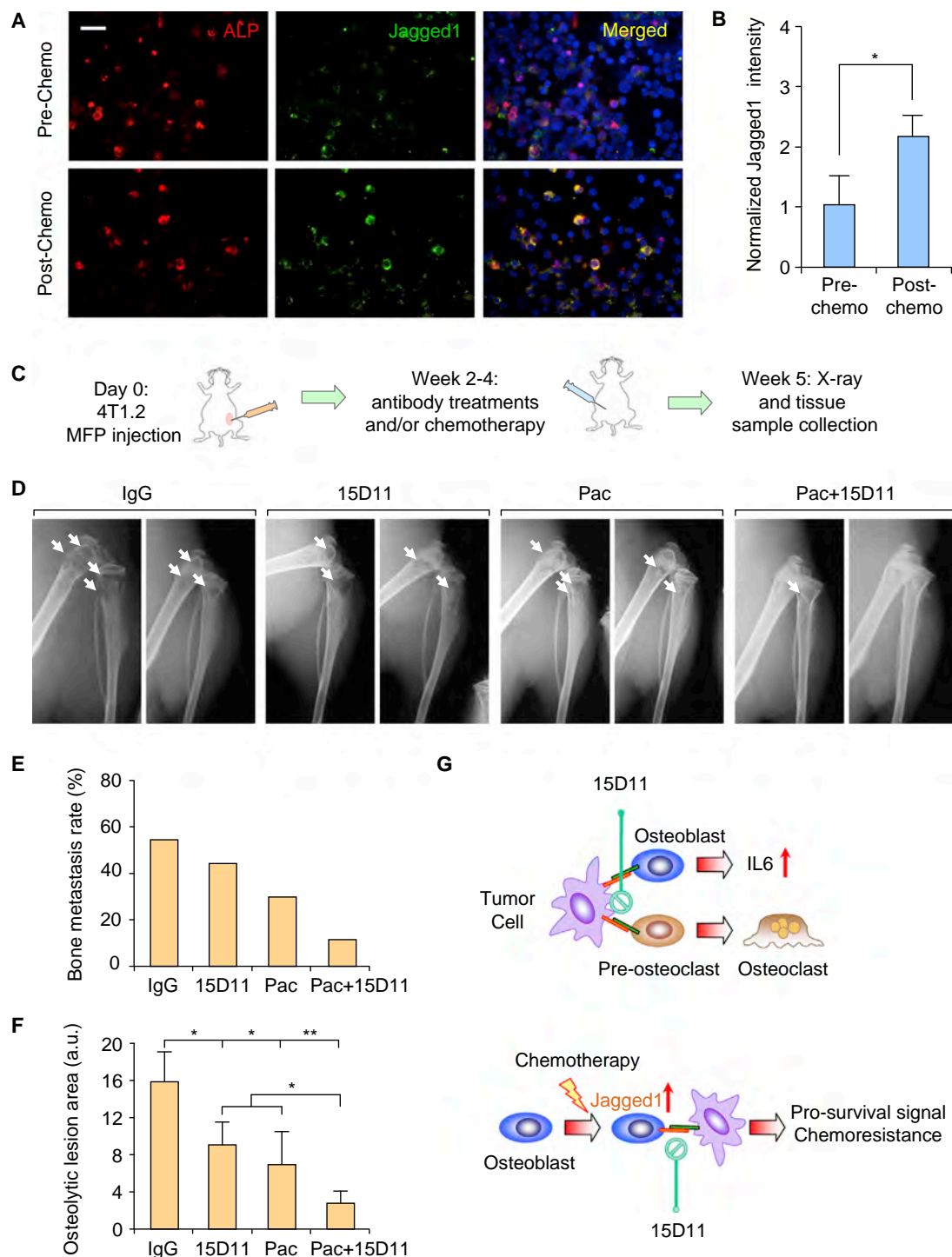
Figure 8. Combination of 15D11 and Chemotherapy Strongly Inhibits Spontaneous Bone Metastasis

(A) Paired bone marrow cytospin samples were collected from cancer patients before and after cisplatin + paclitaxel chemotherapy. Slides were IF co-stained for ALP+ osteoblasts (red) and Jagged1 (green). Scale bar, 40 μm.

(B) Normalized signal intensity of Jagged1 staining to ALP staining. Signal intensity was quantified using ImageJ software (NIH). n = 14 samples per group; data presented as mean ± SEM. *p < 0.05 by Student's t test.

(C) Schematic representation of experimental procedures. 4T1.2 mouse mammary tumor cells were injected in the mammary fat pad of 6–8-week-old female BALB/c mice. Two weeks later when the primary tumors progressed to about 5–8 mm in diameter, mice were treated with IgG, 15D11 (10 mg/kg), paclitaxel (20 mg/kg), or both 15D11 and paclitaxel, twice a week. Spontaneous bone metastasis progression was monitored by weekly X-ray images and by histological H&E staining and TRAP staining. n = 10 for each experimental group.

(legend continued on next page)

underscore the importance of improving the efficacy of adjuvant chemotherapy. Our current study indicates that chemotherapy-induced Jagged1 in osteoblasts may provide a pro-survival niche for DTCs, and targeting a Jagged1-mediated niche may increase the elimination of DTCs by chemotherapy and reduce bone metastasis. As a proof-of-concept of such combined treatment strategy, spontaneous bone metastasis from the murine 4T1.2 mammary tumors were drastically reduced after combined chemotherapy and 15D11 treatment. Given the excellent safety profile of 15D11, it represents an ideal agent for further clinical development both for the treatment of established bone metastasis and for preventing relapse in early-stage breast and other cancers that frequently metastasize to bone.

STAR★METHODS

Detailed methods are provided in the online version of this paper and include the following:

- KEY RESOURCES TABLE
- CONTACT FOR REAGENT AND RESOURCE SHARING
- EXPERIMENTAL MODEL AND SUBJECT DETAILS
  - Animal Models
  - Clinical Bone Marrow Cytospin Analysis
  - Cell Lines
- METHOD DETAILS
  - Osteoclast Differentiation Assay
  - 2-D and 3-D Tumor-Stromal Co-Culture
  - Labeling of MC3T3 and MSC Cells
  - Generation and Characterization of 15D11 Antibody
  - *In Vivo* Treatment Schedule and Dosing
  - Effect of 15D11 Antibody on Angiogenesis
  - Bone Histology Analysis
  - μCT Analysis
  - X-Ray Imaging and Osteolytic Lesion Quantification
  - Western Blot Analyses
  - RNA Isolation and qRT-PCR Analysis
  - Microarray and Heatmap Generation
- QUANTIFICATION AND STATISTICAL ANALYSIS
- DATA AND SOFTWARE AVAILABILITY

SUPPLEMENTAL INFORMATION

Supplemental Information includes seven figures, one table, and six movies and can be found with this article online at https://doi.org/10.1016/j.ccell.2017.11.002.

AUTHOR CONTRIBUTIONS

Conceptualization, H.Z., Y.B., H.T.J., A.C., B.L., Y.K.; Methodology, H.Z., Y.B., S.K., G.R., M.E., Y.W., H.T.J., A.C., B.L., Y.K.; Software, H.Z., Y.B., L.Z.; Validation, Y.W., S.K., M.S., M.E., H.Z., Y.B., A.C., B.L., Y.K. ; Formal Analysis, H.Z., Y.B., W.L., Y.W., S.K., L.Z., N.T., B.L., Y.K.; Investigation, H.Z., Y.B., S.K., R.T., J.C., G.R., M.Y., M.E., W.L., Y.W., M.S., C.K., J.S., J.M., H.T.J.;

Resources, S.K., N.T., K.P., A.C., B.L., Y.K.; Data Curation, H.Z., Y.B., Y.W., C.K., J.S., J.M., H.T.J., A.C., B.L., Y.K.; Writing – Original Draft, H.Z., Y.K.; Writing – Review & Editing, H.Z., Y.B., H.T.J., H.T.J., A.C., B.L., Y.K.; Visualization, H.Z., Y.K.; Supervision, A.C., B.L., Y.K.; Project Administration, H.Z., Y.B., A.C., B.L., Y.K.; Funding Acquisition, A.C. B.L., Y.K.

REFERENCES

Anampa, J., Makower, D., and Sparano, J.A. (2015). Progress in adjuvant chemotherapy for breast cancer: an overview. BMC Med. *13*, 195.

Benedito, R., Roca, C., Sorensen, I., Adams, S., Gossler, A., Fruttiger, M., and Adams, R.H. (2009). The notch ligands Dll4 and Jagged1 have opposing effects on angiogenesis. Cell *137*, 1124–1135.

Braun, S., Vogl, F.D., Naume, B., Janni, W., Osborne, M.P., Coombes, R.C., Schlimok, G., Diel, I.J., Gerber, B., Gebauer, G., et al. (2005). A pooled analysis of bone marrow micrometastasis in breast cancer. N. Engl. J. Med. *353*, 793–802.

Cao, Z., Ding, B.S., Guo, P., Lee, S.B., Butler, J.M., Casey, S.C., Simons, M., Tam, W., Felsher, D.W., Shido, K., et al. (2014). Angiocrine factors deployed by tumor vascular niche induce B cell lymphoma invasiveness and chemoresistance. Cancer Cell *25*, 350–365.

Dotto, G.P. (2009). Crosstalk of Notch with p53 and p63 in cancer growth control. Nat. Rev. Cancer *9*, 587–595.

Duan, C.W., Shi, J., Chen, J., Wang, B., Yu, Y.H., Qin, X., Zhou, X.C., Cai, Y.J., Li, Z.Q., Zhang, F., et al. (2014). Leukemia propagating cells rebuild an evolving niche in response to therapy. Cancer Cell *25*, 778–793.

Eckhardt, B.L., Parker, B.S., van Laar, R.K., Restall, C.M., Natoli, A.L., Tavaria, M.D., Stanley, K.L., Sloan, E.K., Moseley, J.M., and Anderson, R.L. (2005). Genomic analysis of a spontaneous model of breast cancer metastasis to bone reveals a role for the extracellular matrix. Mol. Cancer Res. *3*, 1–13.

(D) X-ray images of these experimental mice at week 5. Arrows indicate osteolytic bone areas.
(E) Quantification of the percentage of mice that developed spontaneous bone metastasis based on X-ray and H&E staining at the endpoint.
(F) Quantification of osteolytic lesions based on X-ray images. n = 8; data presented as mean ± SEM. *p < 0.05, **p < 0.01 by Student's t test.
(G) Schematic model for Jagged1-Notch signaling in bone metastasis progression and chemoresistance. Tumor-derived Jagged1 promote bone metastasis by engaging osteoblasts and osteoclasts (upper panel), while chemotherapy-induced Jagged1 in osteogenic cells promotes tumor cell survival under chemotherapy (lower panel). 15D11 targets both processes and synergizes with chemotherapy to strongly reduce bone metastasis.

Ell, B., Mercatali, L., Ibrahim, T., Campbell, N., Schwarzenbach, H., Pantel, K., Amadori, D., and Kang, Y. (2013). Tumor-induced osteoclast miRNA changes as regulators and biomarkers of osteolytic bone metastasis. Cancer Cell *24*, 542–556.

Forozan, F., Veldman, R., Ammerman, C.A., Parsa, N.Z., Kallioniemi, A., Kallioniemi, O.P., and Ethier, S.P. (1999). Molecular cytogenetic analysis of 11 new breast cancer cell lines. Br. J. Cancer *81*, 1328–1334.

Gu, B., Espana, L., Mendez, O., Torregrosa, A., and Sierra, A. (2004). Organ-selective chemoresistance in metastasis from human breast cancer cells: inhibition of apoptosis, genetic variability and microenvironment at the metastatic focus. Carcinogenesis *25*, 2293–2301.

Hanoun, M., Zhang, D., Mizoguchi, T., Pinho, S., Pierce, H., Kunisaki, Y., Lacombe, J., Armstrong, S.A., Duhrsen, U., and Frenette, P.S. (2014). Acute myelogenous leukemia-induced sympathetic neuropathy promotes malignancy in an altered hematopoietic stem cell niche. Cell Stem Cell *15*, 365–375.

Imbimbo, B.P. (2008). Therapeutic potential of gamma-secretase inhibitors and modulators. Curr. Top. Med. Chem. *8*, 54–61.

Kang, Y., Siegel, P.M., Shu, W., Drobnjak, M., Kakonen, S.M., Cordon-Cardo, C., Guise, T.A., and Massague, J. (2003). A multigenic program mediating breast cancer metastasis to bone. Cancer Cell *3*, 537–549.

Kellermann, S.A., and Green, L.L. (2002). Antibody discovery: the use of transgenic mice to generate human monoclonal antibodies for therapeutics. Curr. Opin. Biotechnol. *13*, 593–597.

Kos, C.H., Karaplis, A.C., Peng, J.B., Hediger, M.A., Goltzman, D., Mohammad, K.S., Guise, T.A., and Pollak, M.R. (2003). The calcium-sensing receptor is required for normal calcium homeostasis independent of parathyroid hormone. J. Clin. Invest. *111*, 1021–1028.

Li, D., Masiero, M., Banham, A.H., and Harris, A.L. (2014). The notch ligand JAGGED1 as a target for anti-tumor therapy. Front. Oncol. *4*, 254.

Lu, J., Ye, X., Fan, F., Xia, L., Bhattacharya, R., Bellister, S., Tozzi, F., Sceusi, E., Zhou, Y., Tachibana, I., et al. (2013). Endothelial cells promote the colorectal cancer stem cell phenotype through a soluble form of Jagged-1. Cancer Cell *23*, 171–185.

Mendez, M.J., Green, L.L., Corvalan, J.R., Jia, X.C., Maynard-Currie, C.E., Yang, X.D., Gallo, M.L., Louie, D.M., Lee, D.V., Erickson, K.L., et al. (1997). Functional transplant of megabase human immunoglobulin loci recapitulates human antibody response in mice. Nat. Genet. *15*, 146–156.

Miller, A.C., Lyons, E.L., and Herman, T.G. (2009). cis-Inhibition of Notch by endogenous Delta biases the outcome of lateral inhibition. Curr. Biol. *19*, 1378–1383.

Paul, M.K., Bisht, B., Darmawan, D.O., Chiou, R., Ha, V.L., Wallace, W.D., Chon, A.T., Hegab, A.E., Grogan, T., Elashoff, D.A., et al. (2014). Dynamic changes in intracellular ROS levels regulate airway basal stem cell homeostasis through Nrf2-dependent Notch signaling. Cell Stem Cell *15*, 199–214.

Pitt, L.A., Tikhonova, A.N., Hu, H., Trimarchi, T., King, B., Gong, Y., Sanchez-Martin, M., Tsirigos, A., Littman, D.R., Ferrando, A.A., et al. (2015). CXCL12-producing vascular endothelial niches control acute T cell leukemia maintenance. Cancer Cell *27*, 755–768.

Polverino, A., Coxon, A., Starnes, C., Diaz, Z., DeMelfi, T., Wang, L., Bready, J., Estrada, J., Cattley, R., Kaufman, S., et al. (2006). AMG 706, an oral, multikinase inhibitor that selectively targets vascular endothelial growth factor, platelet-derived growth factor, and kit receptors, potently inhibits angiogenesis and induces regression in tumor xenografts. Cancer Res. *66*, 8715–8721.

Reedijk, M., Odorcic, S., Chang, L., Zhang, H., Miller, N., McCready, D.R., Lockwood, G., and Egan, S.E. (2005). High-level coexpression of JAG1 and NOTCH1 is observed in human breast cancer and is associated with poor overall survival. Cancer Res. *65*, 8530–8537.

Ren, G., Zhang, L., Zhao, X., Xu, G., Zhang, Y., Roberts, A.I., Zhao, R.C., and Shi, Y. (2008). Mesenchymal stem cell-mediated immunosuppression occurs via concerted action of chemokines and nitric oxide. Cell Stem Cell *2*, 141–150.

Ridgway, J., Zhang, G., Wu, Y., Stawicki, S., Liang, W.C., Chanthery, Y., Kowalski, J., Watts, R.J., Callahan, C., Kasman, I., et al. (2006). Inhibition of Dll4 signalling inhibits tumour growth by deregulating angiogenesis. Nature *444*, 1083–1087.

Rizzo, P., Osipo, C., Foreman, K., Golde, T., Osborne, B., and Miele, L. (2008). Rational targeting of Notch signaling in cancer. Oncogene *27*, 5124–5131.

Sethi, N., Dai, X., Winter, C.G., and Kang, Y. (2011). Tumor-derived JAGGED1 promotes osteolytic bone metastasis of breast cancer by engaging notch signaling in bone cells. Cancer Cell *19*, 192–205.

Shiozawa, Y., Pedersen, E.A., Havens, A.M., Jung, Y., Mishra, A., Joseph, J., Kim, J.K., Patel, L.R., Ying, C., Ziegler, A.M., et al. (2011). Human prostate cancer metastases target the hematopoietic stem cell niche to establish footholds in mouse bone marrow. J. Clin. Invest. *121*, 1298–1312.

Sprinzak, D., Lakhanpal, A., Lebon, L., Santat, L.A., Fontes, M.E., Anderson, G.A., Garcia-Ojalvo, J., and Elowitz, M.B. (2010). cis-Interactions between Notch and Delta generate mutually exclusive signalling states. Nature *465*, 86–90.

Wan, L., Lu, X., Yuan, S., Wei, Y., Guo, F., Shen, M., Yuan, M., Chakrabarti, R., Hua, Y., Smith, H.A., et al. (2014). MTDH-SND1 interaction is crucial for expansion and activity of tumor-initiating cells in diverse oncogene- and carcinogen-induced mammary tumors. Cancer Cell *26*, 92–105.

Wang, H., Yu, C., Gao, X., Welte, T., Muscarella, A.M., Tian, L., Zhao, H., Zhao, Z., Du, S., Tao, J., et al. (2015). The osteogenic niche promotes early-stage bone colonization of disseminated breast cancer cells. Cancer Cell *27*, 193–210.

Weilbaecher, K.N., Guise, T.A., and McCauley, L.K. (2011). Cancer to bone: a fatal attraction. Nat. Rev. Cancer *11*, 411–425.

STAR★METHODS

KEY RESOURCES TABLE

REAGENT or RESOURCE	SOURCE	IDENTIFIER
Antibodies		
Alkaline Phosphatase/ALPL in 1:100, Rat	R & D Systems	Cat# MAB29091; RRID:AB_11129451
beta Actin [AC-15] in 1:10,000, Mouse	Abcam	Cat# ab6276; RRID:AB_2223210
Cleaved Caspase-3 (Asp175)	Cell Signaling Technology	Cat# 9661; RRID:AB_2341188
GFP in 1:1,000, Chicken	Abcam	Cat# ab13970; RRID:AB_300798
Jagged1(H114) in 1:1,000, Rabbit	Santa Cruz Biotechnology	Cat# sc-8303; RRID:AB_649685
Jagged1 in 1:100 (IF), Rabbit	Acris Antibodies	Cat# AP09127PU-N; RRID:AB_2035312
Ki67 in 1:100, Rabbit	Abcam	Cat# ab15580; RRID:AB_443209
IL6 in 1:1,000, Rabbit	MBL International	Cat# JM-5144-100; RRID:AB_592035
PARP in 1:1,000, Rabbit	Cell Signaling Technology	Cat# 9542; RRID:AB_2160739
15D11 fully human anti-human Jagged1 antibody	Amgen Inc.	N/A
Anti-Rabbit IgG - Horseradish Peroxidase in 1:5,000, Goat	GE Healthcare	Cat# RPN4301; RRID:AB_2650489
Anti-Mouse IgG - Horseradish Peroxidase in 1:5,000, Sheep	GE Healthcare	Cat# NA931-1ml; RRID:AB_772210
Bacterial and Virus Strains		
pMSCV-Puro	Sethi et al., 2011	NA
pMSCV-Jagged1	Sethi et al., 2011	NA
pTyr-Co1a1-mJagged1	This paper	NA
Biological Samples		
14 pairs of bone marrow cytospin samples before and after Carboplatinum and paclitaxel treatment	University Hospital Essen, Essen, Germany	NA
Chemicals, Peptides, and Recombinant Proteins		
OPG-Fc	Amgen Inc.	NA
Brefeldin A	Sigma-Aldrich	Cat# B6542-5MG
CCl$_4$ (Carbon tetrachloride)	Sigma-Aldrich	Cat# 319961
Cisplatin	Sigma-Aldrich	Cat# 134357-100MG
Docetaxel	Sigma-Aldrich	Cat# 1224551-200MG
Hydrogen peroxide solution	Sigma-Aldrich	Cat# 216763
MRK003	Merck	NA
N-Acetyl-L-cysteine	Sigma-Aldrich	Cat# A7250-5G
Paclitaxel	Sigma-Aldrich	Cat# T7191-25MG
(+)-Sodium L-ascorbate	Sigma-Aldrich	Cat# A4034
Tunicamycin	Sigma-Aldrich	Cat# T7765
Recombinant Mouse IL6 Protein	R&D Biosystems	Cat# 406-ML-005
Recombinant Mouse RANKL Protein	R&D Biosystems	Cat# 462-TEC-010
Critical Commercial Assays		
Acid Phosphatase, Leukocyte (TRAP) Kit	Sigma-Aldrich	387A-1KT
ALT Activity Assay	Sigma-Aldrich	MAK052
AST Activity Assay	Sigma-Aldrich	MAK055
Deposited Data		
Gene expression microarray data	GSE97997	https://www.ncbi.nlm.nih.gov/geo/query/acc.cgi?token=cpancgoafjcnxyv&acc=GSE97997
Experimental Models: Cell Lines		
Chinese hamster CHO	ATCC	Cat# CCL-61
Human embryonic kidney H29-Clone#7	Sethi et al., 2011	NA

(Continued on next page)

Continued

REAGENT or RESOURCE	SOURCE	IDENTIFIER
Mouse osteoblast MC3T3-E1 Clone #4	ATCC	Cat# CRL-2393
Mouse mesenchymal stromal cell (MSC)	Ren et al., 2008	NA
Mouse PyMT-A-FIG	Wan et al., 2014	NA
Human breast cancer MCF7	ATCC	Cat# HTB-22
Human breast cancer SCP28	Kang et al., 2003	NA
Human breast cancer SCP2	Kang et al., 2003	NA
Human breast cancer SCP28-Vector	Sethi et al., 2011	NA
Human breast cancer SCP28-Jagged1	Sethi et al., 2011	NA
Human breast cancer SUM1315-M1B1	another manuscript in preparation, derivative from SUM1315	NA
Human embryonic kidney 293T	ATCC	Cat# CRL-3216
Mouse breast cancer 4T1.2	Eckhardt et al., 2005	RRID:CVCL_GR32
Experimental Models: Organisms/Strains		
Mouse Bal/cJ	Jackson Laboratory	Cat# 000651
Mouse FVB/NJ	Jackson Laboratory	Cat# 001800
Mouse nu/nu	Jackson Laboratory	Cat#: 002019
Mouse Col1a1-Jag1 (FVB)	This paper	NA
XenoMouse XMG2KL	Kellermann and Green, 2002	NA
XenoMouse XMG4KL	Kellermann and Green, 2002	NA
Oligonucleotides		
See Table S1 for real-time PCR primers	IDT	NA
Col1a1-Jag1-GT-F	IDT	CAACACCACGGAATTGTCAGT
Col1a1-Jag1-GT-R	IDT	GATGATGGGAACCCTGTCAA
Software and Algorithms		
AxioVision software version 4.6.3	Zeiss	NA
GeneSpring 13 software	Agilent	NA
ImageJ	National Institute of Health	NA
INVEON Research Workplace software	Siemens Healthcare	NA
NIS-Elements Confocal	Nikon	NA
Deposited Data		
Microarray data	GSE97997	Microarray data can be accessed at https://www.ncbi.nlm.nih.gov/geo/query/acc.cgi?token=cpancgoa

CONTACT FOR REAGENT AND RESOURCE SHARING

Further information and requests for resources and reagents should be directed to the Lead Contact Yibin Kang at ykang@princeton.edu.

15D11 antibody is the property of Amgen Inc. and utilized for this study under an MTA. A request for 15D11 antibody needs to be negotiated with Amgen directly.

EXPERIMENTAL MODEL AND SUBJECT DETAILS

Animal Models

All procedures involving mice and experimental protocols were approved by the Institutional Animal Care and Use Committees (IACUC) of Princeton University and Amgen Inc. Mice were purchased from Jackson laboratory with detailed information listed in Key Resources Table. For orthotopic primary tumor formation and spontaneous bone metastasis assay, female BALB/c mice (4-6 weeks old) were anaesthetized and a small incision was made to reveal the mammary gland. 10^5 GFP labeled 4T1.2 tumor cells suspended in 10 μl PBS were injected directly into the mammary fat pad. Spontaneous bone metastasis was monitored by X-ray imaging. Mice were euthanized when the primary tumor reaches 20x20 mm. For experimental bone metastasis, three models were used using intra-cardiac (IC), intra-iliac artery (IIA) and intra-tibia (IT) injection methods. For all these injections, tumor cells

were harvested from subconfluent cell culture, washed with PBS, and suspended at 10^6 cells/ml in PBS for IC and IIA, and at 2.5×10^7 cells/ml in PBS for IT injection. Mice were anesthetized with ketamine (100 mg/kg body weight) and xylazine (10 mg/kg body weight) before injection. For IC injection, 0.1ml cells were injected into the left cardiac ventricle of 4-6 week-old, female athymic nude mice using 26G needles. Successful injection was confirmed by BLI imaging confirming evenly distributed bioluminescent signal in the whole body. For IIA injection, a small incision of about 1.5 cm was made on the skin in the middle line between femoral and ilium bones. Muscles were dissected to reveal iliac artery. Cancer cells in 0.1 ml PBS were injected by 31G superfine insulin needles under the dissecting microscope. The wounded area was then pressed for 10 minutes to stop the bleeding and closed with wound clips before BLI imaging. For IT injection, 4-6 week-old female FVB mice were used. Mouse leg was bended and the skin area was visualized with 70% ethanol wiping. Insert a 28G needle under patella and penetrate the tibial growth plate, slowly press the plunger to inject 10 μl of cell solution. Bone metastasis burden was monitored by weekly BLI and X-ray imaging. At the experimental endpoint, mice were euthanized for bone histology analysis and half of the bone samples were used for μCT imaging and bone density quantification.

The human Jagged1 cDNA was PCR amplified and cloned into the retroviral expression vector pMSCVpuro using XhoI and EcoRI restriction sites. To generate the Col1a1-Jag1 mouse strain, we used a backbone vector of pTyr-Co1a1. Mouse cDNA library was generated using a mouse mammary gland mRNA from FVB background mice and reverse transcribed to cDNA by using SuperScript III First Strand Synthesis System for RT-PCR (118080-051 Life Technologies CA). Jagged1 cDNA was PCR amplified using this library by a pair of primers both with SwaI restriction enzyme overhangs (CATT <u>ATTTAAAT</u>gccaccatgcggtccccacgga and CATT <u>ATTTAAAT</u> ctgctatacgatgtattccatccgg) and inserted into SwaI site of pTyr-Col1a1 plasmid with sequencing confirmation. The genotyping was performed using primer pairs of CAACACCACGGAATTGTCAGT and GATGATGGGAACCCTGTCAA with final PCR product of 1012 bps.

Clinical Bone Marrow Cytospin Analysis

14 pairs of bone marrow cytospin samples (without any DTCs) from cancer patients before and after Carboplatinum and paclitaxel were acquired from the University Hospital Essen, Essen, Germany. Patients were de-identified and were considered exempt by the Institutional Review Boards of Princeton University. Cytospin slides were dried on room temperature for 1 hr before staining. Slides were thawed for 3 min and fixed for 10 min with 4% PFA in PBS before permeabilized in 0.2% Triton X-100 in PBS for 10 min and blocked in 10% goat serum for 20 min. Samples were then incubated with Jagged1 primary antibody for 1 hr and in secondary antibody for 45 min. Samples were blocked for 20 min before incubation with the next set of primary (Alkinine Phosphatase antibody) and secondary antibodies. All antibodies were diluted in 10% goat serum. Slides were stained with Hoechst and mounted with coverslips using Prolong gold antifade reagent.

Cell Lines

293T, 4T1.2, SCP28, SCP28-Vector and -Jagged1 cells, SCP28, RAW264.7, were cultured in DMEM supplemented with 10% FBS, 1% penicillin-streptomycin, and 0.2% Amphotericin B. MCF7 cells were culture in DMEM supplemented with 10% FBS, 1% penicillin-streptomycin, and 0.01 mg/ml Insulin. SUM1315-M1B1 was cultured in F12 medium with 5% FBS, 1% penicillin-streptomycin, 0.2% Amphotericin B, 5 μg/ml insulin, and 10 ng/ml EGF. H29-Clone#7 was cultured in DMEM supplemented with 10% FBS, 1% penicillin-streptomycin, 0.2% Amphotericin B, 0.5 μg/ml doxycycline, 2 μg/ml puromycin, and 300 μg/ml G418. H29-Clone#7 was cultured without all antibiotics when used for retrovirus production. MC3T3-E1 Clone #4 (denoted as MC3T3 for abbreviation thereafter) was cultured in α-MEM with 10% FBS, 1% penicillin-streptomycin, and 0.2% Amphotericin B. Mouse mesenchymal stromal cell (MSC, isolated from Balb/c) was cultured in DMEM supplemented with 10% FBS, 1% penicillin-streptomycin, 0.2% Amphotericin B, and 20 ng/ml FGF. All plasmids were transfected into different cell lines using Lipofectamine 2000 following the manufacturer's manual (Life technologies, CA, USA). To generate stable cell lines, a pLEX-MCS based lentivirus vector or a pMSCV-hygro based retrovirus vector was used in our study. Lentiviruses were packaged in HEK293T cells while retroviruses were packaged by using H29 cell line. Conditioned media from these packaging cells containing viruses were collected 2 days and 3 days after transfection. Recipient cell lines were exposed to conditioned media containing viruses supplemented with 2 μg/mL Polybrene for 48 hr. Infected cells were selected with puromycin or hygromycin to generate stable expressing cell lines. 293T and H29clone#7 are cell lines from female humans. All other cancer cell lines are breast cancer cell lines from either female human or mouse.

METHOD DETAILS

Osteoclast Differentiation Assay

For osteoclast differentiation assays, RAW264.7 cells were seeded onto Fc- or recombinant Jagged1 protein plates, or co-cultured with indicated cell lines at the concentration of 0.2 million cells/well in 12 well plate. Cells were then treated with 5 ng/ml RANKL in DMEM plus 10% FBS, with media changed every 2 days and twice a day from Day 5 and on. Primary pre-osteoclasts were isolated from bone marrow cells flushed from the tibia of 6-week-old WT Balb/c mice and filtered through a 70 μm cell-strainer before overnight culture in α-MEM with 10% FBS. The following day non-adherent cells were plated and supplemented with 50 ng/mL M-CSF for 2 days. Cells were then re-plated onto Fc- or recombinant Jagged1 protein plates, or co-cultured with indicated cell lines in 12 well plate at the presence of 5ng/ml RANKL in DMEM plus 10% FBS, with media changed every 2 days (media was changed twice a day

from Day 5 and on). Mature osteoclasts were TRAP stained using a leukocyte acid phosphatase kit (387A-1KT Sigma) and TRAP positive and multinucleated cells were quantified as mature osteoclasts.

2-D and 3-D Tumor-Stromal Co-Culture

For 2-D tumor osteoblast co-culture, SCP28-vector or SCP28-Jagged1 tumor cells were cultured with MC3T3 cells in 10 cm plate in DMEM with 10% FBS. One day after co-culture, media was changed to serum free DMEM for another 24 hr before the conditioned media collection. The collected conditioned media were concentrated by centrifuging at room temperature at 4000 rpm using Amicon Ultra-15 (3K) centrifuge filter (UFC900324, EMD Millipore, MA, USA) for further usage. For tumor-stroma cell 3-D co-culture assay, 1:1 ratio, a total of 10000 tumor cells and MC3T3 cells (or MSCs) were cultured in a serum free mammosphere formation media in low attachment plates (Corning, Corning NY, USA). The media is freshly prepared with 1 ml B27 (Life Technologies, CA, USA), 20 ng/ml bFGF (Novoprotein, NJ, USA), 20 ng/ml EGF (Novoprotein, NJ, USA), 100 μg/ml Gentamycin (Life Technologies, CA, USA), and 0.25 ml non-essential amino acid solution (Life Technologies, CA, USA) in a total of 50 ml DMEM/F12 media. Cells were cultured to form 3-D spheres before treating with respective chemotherapeutic agent.

Labeling of MC3T3 and MSC Cells

To generate labeled MSC and MC3T3 cells for co-culture study, we infected these two cell lines with pLEX-mCherry lentivirus for two days and let the cells expand for anther 5 days. Cultured cells were then trypsin digested and re-suspended in FACS buffer (PBS supplemented with 5% newborn calf serum) and filtered through 70 mm nylon cell strainers before flow cytometric analysis on a FACS sort instrument (BD Biosciences). Non-labeled parental cells were used as negative control. DAPI was used for nuclear counter staining to eliminate dead cells.

Generation and Characterization of 15D11 Antibody

Immunization

Fully human antibodies to Jagged1 were generated using XenoMouse technology, transgenic mice engineered to express diverse repertoires of fully human IgGκ and IgGλ antibodies of the corresponding isotypes (Kellermann and Green, 2002; Mendez et al., 1997). XMG2-KL and XMG4-KL strains of mice were immunized with CHO transfectants expressing full length human Jagged1. Cellular immunogens were dosed at 4.0×10^6 Jagged1 transfected cells/mouse and subsequent boosts were of 2.0×10^6 Jagged1 transfected cells/mouse. Injection sites used were combinations of subcutaneous base-of-tail and intraperitoneal. Adjuvant used was Alum (E.M. Sergent Pulp and Chemical Co., Clifton, NJ, cat. # 1452-250). Mice were immunized over a period of 8 weeks to 12 weeks.

Antibody Specificity Determination

After 14 days of culture, hybridoma supernatants were screened for human Jagged1 specific monoclonal antibodies by Fluorometric Microvolume Assay Technology (FMAT) (Applied Biosystems, Foster City, CA). The supernatants were screened against 293T cells transiently transfected with human Jagged1 and counter screened against 293T cells transiently transfected with the same expression plasmid that did not contain the *JAG1* gene.

Ligand Binding Affinity Test

A ligand binding competition method was developed to identify antibodies (in the hybridoma supernatants) that bind Jagged1 ligand and block binding of three receptors: Notch-3, Notch 2 and Notch-1. FACS assays were performed by incubating 20 μl of hybridoma supernatants with 50000 cells transiently expressing at 4°C for 1 hr followed by two washes with PBS/BSA. Cells were then treated with 5μg/ml florochrome-labeled Notch-3 (#1559-NT, R&D Systems) at 4°C followed by two washes. The cells were re-suspended in 1ml PBS/BSA and antibody binding was analyzed using a FACS Calibur™ instrument. Similar assays were performed using Notch-2 (#3735-NT, R&D Systems) and Notch-1 (#3647-TK, R&D Systems).

   The experiments included negative control hybridoma supernatants. The average signal observed in these negative control experiments was adopted as the maximum possible signal for the assay. Experimental supernatants were compared to this maximum signal and a percent inhibition was calculated for each well (% Inhibition = (1-(FL1 of the anti-BCMA hybridoma supernatant/ Maximum FL1 signal))).

Additional Binding Characterization

FACS binding assays were performed to evaluate the binding of the anti-Jagged1 specific antibodies to the murine Jagged1 as well as related Notch ligands, human Jagged2 and human Dll4. FACS assays were performed by incubating hybridoma supernatants with 50000 cells at 4°C for 1 hr followed by two washes with PBS/BSA. Cells were then treated with florochrome-labeled secondary antibodies at 4°C followed by two washes. The cells were re-suspended in 1 ml PBS/BSA and antibody binding was analyzed using a FACSCalibur™ instrument.

K_d Estimation by KinExA

Binding of anti-Jagged1 antibody 15D11 with 293T/muJagged1 clone1 cells were tested on KinExA. Briefly, UltraLink Biosupport (Pierce cat# 53110) was pre-coated with goat-anti-huFc (Jackson Immuno Research cat# 109-005-098) and blocked with BSA. 10 pM and 100 pM of Ab 15D11 was incubated with various density (1.5×10^2 - 9.0×10^6 cell / ml) of 293T cells expressing muJagged1 in 1% FBS, 0.05% sodium azide, DMEM. Samples containing 15D11 antibody and whole cells were rocked for 4 hr at room temperature. The whole cells and antibody-cell complexes were separated from unbound free antibody using Beckman GS-6R centrifuge at approximately 220 *g* for 5 min. The supernatant was filtered through 0.22 μm-filter before passing the goat-anti-huFc-coated beads.

The amount of the bead-bound Ab 15D11 was quantified by fluorescent (Cy5) labeled goat anti-humanIgG (H+L) antibody (Jackson Immuno Research cat# 109-175-088). The binding signal is proportional to the concentration of free Ab 15D11 in solution at each cell density. Equilibrium dissociation constant (K_d) was estimated using model of unknown ligand for n-curve analysis in KinExA™ Pro software.

In Vivo Treatment Schedule and Dosing

The initial treatment is either one day before tumor cell injection or one week after tumor cell injection as described in each experiment. For IgG or 15D11 antibody treatment, mice were intraperitoneal (i.p.) injected at the dosing of 10 mg/kg, twice a week. For OPG-Fc treatment, mice were i.p. injected at the dosing of 3 mg/kg, twice a week. For paclitaxel treatment, paclitaxol powder was first dissolved in 95% ethanol, sonicated and shaked overnight, before mixed 1:1 with cremophor (Sigma Catalog#: 769193-1KG) to reach the final concentration of 20 mg/ml. Paclitacel was diluted 5 times in PBS right before usage. Mice were i.v. injected at 25 mg/kg for the first time, and then 20 mg/kg each time, twice a week for up to total of 6 times. Cisplatin was used at the dosing of 2 mg/kg in experiment in Figure 5D. For treatment using GSI inhibitor (MRK003), mice were administered either the vehicle control (0.5% methylcellulose) or GSI (freshly dissolved in 0.5% methycellulose before each use) by oral gavage twice a week at a 100 mg/kg dosage. The dosing schedule was 2-days ON, 5-days OFF.

Effect of 15D11 Antibody on Angiogenesis

The angiogenesis effect of 15D11 antibody is determined by two methods: 1) Mouse neonatal retina study. Mouse retinas were harvested, stained and fixed as described similarly in a previous study (Ridgway et al., 2006); and 2) Tumor angiogenesis model. 2×10^6 Colo 205 cells were implanted into female athymic nude mice subcutaneously. Mice were randomized at Day 11 before treated with IgG or 15D11 antibody at the dosage of 300μg/mouse for twice a week. Tumor volume was monitored by palpation. To determine tumor angiogenesis effect, Colo205 tumors from mice treated for 96 hr with 500 μg of IgG, or 15D11 antibody were collected. Intra-tumor blood vessels were visualized by CD31 staining and counterstained with hematoxylin. (n = 3 per group). No vascular differences between groups were observed.

Bone Histology Analysis

Hindlimb bones were excised from mice at the end point of each experiment, immediately after the last BLI time point. Following this, the tumor-bearing hind limb bones were fixed in 10% neutral-buffered formalin, decalcified in 10% EDTA for 2 weeks, and embedded in paraffin for hematoxylin and eosin (H&E), tartrate-resistant acid phosphatase (TRAP) (Kos et al., 2003), or immunohistochemical staining. Histomorphometric analysis was performed on H&E stained bone metastasis samples using the Zeiss Axiovert 200 microscope and the AxioVision software version 4.6.3 SP1. For quantitative analysis of lesion area, a 10x objective was used to focus on the tumor region of interest and images were acquired using the AxioCamICc3 camera set to an exposure of around 100 ms. Osteoclast number was assessed as multinucleated TRAP+ cells and reported as number/field. For immunofluorescence staining of the bone samples, Hind limb bones were excised from mice at the end point of each experiment immediately followed by PBS and 4% freshly prepared paraformaldehyde. Non-decalcified bone samples were then frozen in embedding media and sectioned with Leica CM3050S Research Cryostat at 20 μM with Cryofilm type IIIC (Section-Lab, Japan) and stained with respective primary antibodies and fluorophore labeled secondary antibodies. GFP antibody: Cat# ab13970 (Abcam). Jagged1 antibody: Cat# AP09127PU-N (Acris Antibodies). ALP antibody: Cat# MAB29091 (R&D Systems). Cleaved Caspase-3 antibody: Cat# 9661S (Cell Signaling). Ki67 antibody: Cat# ab15580 (Abcam). Images were taken using Nikon A1 confocal microscope at Princeton University Molecular Biology Confocal microscope core facility.

μCT Analysis

Femurs and tibias were scanned using the INVEON PET/CT (Siemens Healthcare) at the Preclinical Imaging Shared Resource of Cancer Institute of New Jersey. The X-Ray tube settings were 80 kV and 500 μA and images were acquired at the highest resolution without CCD binning, resulting in a voxel size of 9.44 μm. A 0.66° rotation step through a 195° angular range with 6500 ms exposure was used. The images were reconstructed with Beam Hardening Correction and Hounsfield calibration before being analyzed using the INVEON Research Workplace software (Siemens Healthcare). After processing with a 3-D Gaussian filter to reduce noise, ROI's were manually segmented that corresponded to the cortical and trabecular bone regions.

X-Ray Imaging and Osteolytic Lesion Quantification

Osteolytic bone lesions in mice were assessed by X-ray radiography. Anesthetized mice were placed on individually wrapped films (BIOMAX XAR Film, Cat#: F5763-50EA, Sigma-Aldrich) and exposed to X-ray radiography at 35 kV for 15 seconds using a MX-20 Faxitron instrument. Films were developed using a Konica SRX-101A processor. Changes in bone remodeling and osteolytic lesions (radiolucent lesions) in the hind limbs of mice were identified and quantified using the Adobe Photoshop software (Adobe Systems Inc.)

Western Blot Analyses

SDS lysis buffer (0.05 mM Tris-HCl, 50 mM BME, 2% SDS, 0.1% Bromophenol blue, 10% glycerol) was used to collect protein from cells. Samples were heat denatured and equally loaded, separated on a 10% SDS-page gel, transferred onto a PVDF membrane

(Millipore), and blocked with 5% milk. Primary antibodies for immunoblotting included: anti-β-actin (1:10,000 dilution, Abcam, cat#ab6276, clone AC-15), anti-Cleaved Caspase 3 (1:1000 dilution, Cell Signaling, Cat# 9661S), anti- IL6 (1:1000 dilution, MLB International Cooperation, cat#JM-5144-100), anti-PARP (1:1000 dilution, Cell Signaling, Cat#9532S), anti-Jagged1 (1:1,000 dilution, Santa Cruz Biotechnology, Cat#SC8303). Membranes were incubated with horseradish peroxidase (HRP)-conjugated anti-mouse, rabbit or rat secondary antibody (1:2,000 dilution, GE Healthcare) for 1 hr and chemiluminescence signals were detected by ECL substrate (GE Healthcare).

RNA Isolation and qRT-PCR Analysis

Total RNAs were isolated from cells using RNeasy kit (Qiagen) following manufacturer's instructions. RNAs were reverse transcribed into cDNAs by using Superscript III reverse transcription kit (Invitrogen). Real-time RT-PCR was performed on ABI 7900 96 HT series PCR machine (Applied Biosystem) using SYBR Green Supermix (Bio-Rad Laboratories). The gene-specific primer sets were used at a final concentration of 0.5 μM. All real-time RT-PCR assays were performed in duplicate in at least two independent experiments. Relative expression values of each target gene were normalized to *GAPDH/Gapdh* mRNA level. The primers used are listed in the Table S1.

Microarray and Heatmap Generation

SUM1315-M1B1 breast cancer cells (GFP labeled) were cultured alone or co-cultured with MC3T3-E1 clone #4 bone osteoblast cells, and treated with control PBS or 10 μM cisplatin for 48 hr. Tumor cells were sorted using FACS based on GFP labeling.

RNA was collected from these samples using the RNAeasy Mini Kit (Qiagen, Valencia VA) according to manufacturer's instructions. The gene expression profiles were determined using Agilent whole human genome microarray 4x44K G4112F, following the manufacturer's instructions. Briefly, the RNA samples and universal human reference RNA (Agilent 740000) were labeled with CTP-cy5 and CTP-cy3, respectively, using the Agilent Quick Amp Labeling Kit. Labeled testing and reference RNA samples were mixed in equal proportions, and hybridized to the human GE 4x44K array. The arrays were scanned with an Agilent G2505C scanner and raw data was extracted using Agilent Feature Extraction software (v11.0). Data was analyzed using the GeneSpring 13 software (Agilent). The expression value of individual probes refers to the Log2(Cy5/Cy3) ratio. The microarray dataset is deposited in GEO database with accession number GSE97997.

Heat map representation of microarray data displays the selected pro- and anti-apoptosis genes from Hallmark-apoptosis signature in MsigDB (http://software.broadinstitute.org/gsea/msigdb/cards/HALLMARK_APOPTOSIS.html). The gene expression values of these genes are further transformed based on median of samples from paired culture conditions (alone vs co-culture) in both saline and cisplatin treatments.

QUANTIFICATION AND STATISTICAL ANALYSIS

Results were reported as mean ± SD (standard deviation) or mean ± SE (standard error of the mean), as indicated in the figure legend. Statistical comparisons were performed using unpaired two-sided Student's t-test with unequal variance assumption and by Mann-Whitney U test. All *in vitro* experiments were repeated three times and animal experiments were repeated once. All the experiments with representative images (including western blot and immunofluorescence) have been repeated at least twice and representative images were shown (except for bone marrow samples). The IF images in Figure 8 are representative of bone marrow cytospin specimens of the same category (pre-treatment vs post-treatment). Quantification of these IF images was performed using ImageJ software.

DATA AND SOFTWARE AVAILABILITY

All microarray data generated in this study have been deposited as a superseries at the NCBI Gene Expression Omnibus with the accession code GSE97997, and can be accessed at https://www.ncbi.nlm.nih.gov/geo/query/acc.cgi?token=cpancgoafjcnxyv&acc=GSE97997.